AGU PUBLICATIONS

Journal of Advances in Modeling Earth Systems

RESEARCH ARTICLE

10.1002/2017MS001154

Precipitation Dynamical Downscaling Over the Great Plains

Xiao-Ming Hu[1,2], Ming Xue[1,2], Renee A. McPherson[3,4], Elinor Martin[2], Derek H. Rosendahl[3], and Lei Qiao[5]

[1]Center for Analysis and Prediction of Storms, University of Oklahoma, Norman, Oklahoma, USA, [2]School of Meteorology, University of Oklahoma, Norman, Oklahoma, USA, [3]South Central Climate Science Center, University of Oklahoma, Norman, Oklahoma, USA, [4]Department of Geography and Environmental Sustainability, University of Oklahoma, Norman, Oklahoma, USA, [5]Department of Natural Resource Ecology and Management, Oklahoma State University, Stillwater, Oklahoma, USA

Key Points:
- The downscaling obtained from this study captures well the spatial/temporal variation of monthly climatology precipitation
- Different cumulus schemes lead to more pronounced difference in simulated rainfall than other tested physics schemes at a 20 km resolution
- Spectral nudging is important for correctly downscaling precipitation over the Great Plains

Supporting Information:
- Supporting Information S1

Correspondence to:
X.-M. Hu,
xhu@ou.edu

Citation:
Hu, X.-M., Xue, M., McPherson, R. A., Martin, E., Rosendahl, D. H., & Qiao, L. (2018). Precipitation dynamical downscaling over the Great Plains. *Journal of Advances in Modeling Earth Systems*, *10*, 421–447. https://doi.org/10.1002/2017MS001154

Received 24 AUG 2017
Accepted 17 JAN 2018
Accepted article online 19 JAN 2018
Published online 9 FEB 2018

Abstract Detailed, regional climate projections, particularly for precipitation, are critical for many applications. Accurate precipitation downscaling in the United States Great Plains remains a great challenge for most Regional Climate Models, particularly for warm months. Most previous dynamic downscaling simulations significantly underestimate warm-season precipitation in the region. This study aims to achieve a better precipitation downscaling in the Great Plains with the Weather Research and Forecast (WRF) model. To this end, WRF simulations with different physics schemes and nudging strategies are first conducted for a representative warm season. Results show that different cumulus schemes lead to more pronounced difference in simulated precipitation than other tested physics schemes. Simply choosing different physics schemes is not enough to alleviate the dry bias over the southern Great Plains, which is related to an anticyclonic circulation anomaly over the central and western parts of continental U.S. in the simulations. Spectral nudging emerges as an effective solution for alleviating the precipitation bias. Spectral nudging ensures that large and synoptic-scale circulations are faithfully reproduced while still allowing WRF to develop small-scale dynamics, thus effectively suppressing the large-scale circulation anomaly in the downscaling. As a result, a better precipitation downscaling is achieved. With the carefully validated configurations, WRF downscaling is conducted for 1980–2015. The downscaling captures well the spatial distribution of monthly climatology precipitation and the monthly/yearly variability, showing improvement over at least two previously published precipitation downscaling studies. With the improved precipitation downscaling, a better hydrological simulation over the trans-state Oologah watershed is also achieved.

1. Introduction

The U.S. Great Plains is known for frequent hazardous convective weather and climate extremes (Feng et al., 2016; Garbrecht et al., 2004; Garbrecht & Rossel, 2002). Across this region, climate change is expected to cause more severe droughts, more intense heavy rainfall events, and subsequently more flooding episodes (Gleason et al., 2008; Groisman & Knight, 2008; Harding & Snyder, 2014; Prein et al., 2017; Shafer et al., 2014; Steiner et al., 2014; Zhang et al., 2013). These potential changes in climate will adversely affect habitats, ecosystems, and landscapes as well as the fish and wildlife they support. Better projections of future, regional precipitation can help natural resource managers mitigate and adapt to these adverse impacts (García-Valdecasas Ojeda et al., 2017; Singh et al., 2013; Soares et al., 2012).

Warm-season convective precipitation is a major driver of the hydrological cycle across the Great Plains (Carbone & Tuttle, 2008; Changnon, 2001). Eastward propagation of moist convection initiated in the Rocky Mountains contributes most to the total precipitation in the Great Plains (Davis et al., 2003; Klein et al., 2006; Leung & Gao, 2016; Pei et al., 2014). Thus the peak time for warm-season climatological precipitation ranges from afternoon in the Rockies to early morning in the eastern Great Plains (e.g., Figure 1a). Convection across the Great Plains is difficult to predict accurately, especially when using today's global climate models (GCMs) with coarse resolutions (Harding et al., 2013; Klein et al., 2006; Leung & Gao, 2016). After Dickinson et al. (1989) and Giorgi (1990), it is now commonly accepted that higher-resolution regional climate information can be obtained by dynamically downscaling coarse-resolution GCM outputs using Regional Climate Models (RCMs). Higher-resolution RCMs have been shown to be able to replicate the temporal and spatial

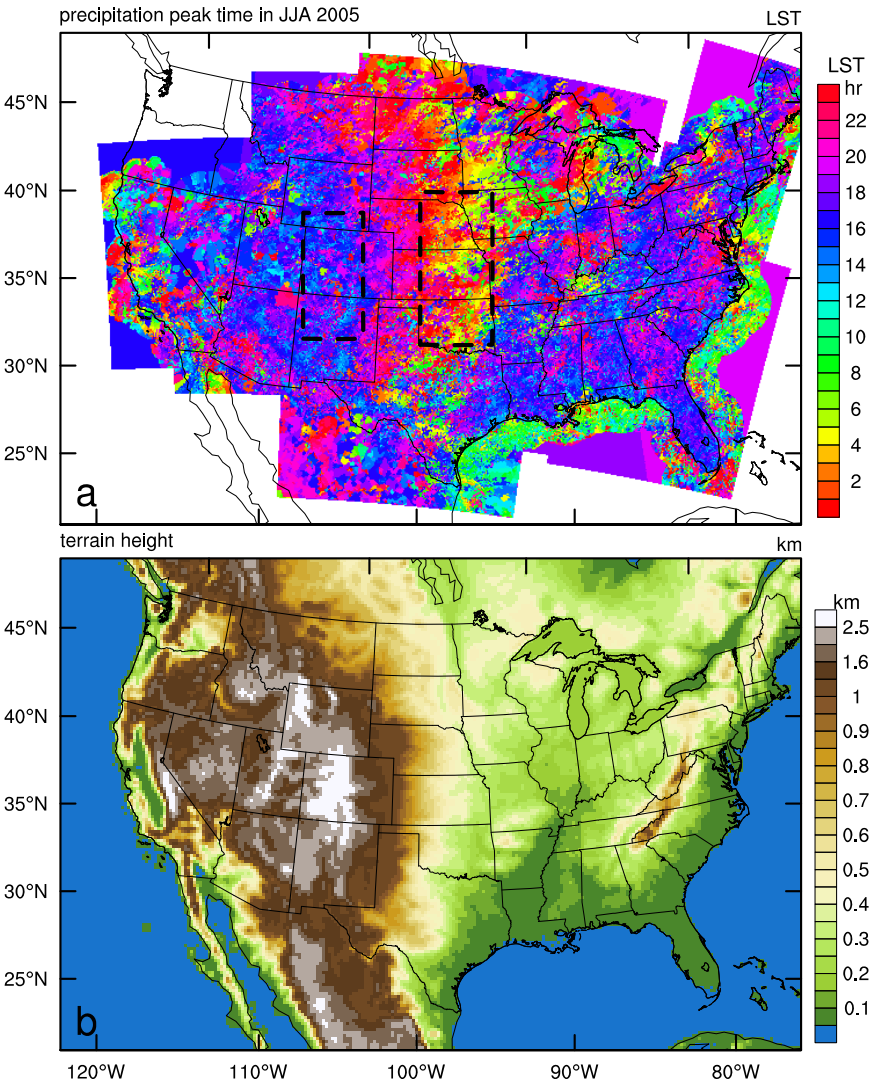

Figure 1. (a) Precipitation peak time (in Local Standard Time, LST) in JJA 2005 calculated from the Stage IV precipitation data and (b) terrain height in the WRF modeling domain. The two rectangular boxes in plot (a) mark the areas of Rockies and Great Plains over where the diurnal variation of precipitation is examined and statistics of simulated precipitation are calculated.

distributions of convective weather during limited time periods for specific regions (Gensini & Mote, 2014). However, in general, there exist large uncertainties with dynamic downscaling. RCMs have been found to be sensitive to spatial resolution (Lee et al., 2007b; Tripathi & Dominguez, 2013; Yamada et al., 2012), nudging strategies (Bowden et al., 2012, 2013; Bullock et al., 2014; Harkey & Holloway, 2013; Liu et al., 2012; Miguez-Macho et al., 2004, 2005; Omrani et al., 2013; Otte et al., 2012; Spero et al., 2014; Wang & Kotamarthi, 2013, 2014), model reinitialization frequency (Lo et al., 2008; Pan et al., 1999; Qian et al., 2003), and physics parameterizations such as cumulus schemes (Choi et al., 2015; Gochis et al., 2002; Liang et al., 2004a, 2004b; Pohl et al., 2014; Qiao & Liang, 2016) and land surface models (Bukovsky & Karoly, 2009; Chen et al., 2014; Vidale et al., 2003). Given these uncertainties, confidence in RCM-downscaled projections of future climate can only be achieved when the credibility of RCM downscaling of historical climate has been proven (Gutowski et al., 2010; Harding & Snyder, 2014; Kendon et al., 2012; Liang et al., 2006; Mearns et al., 2012; Wehner, 2013; Xue et al., 2014).

Our previous dynamical downscaling of historical precipitation over the Great Plains for 2000–2009 using the Weather Research and Forecasting (WRF) model (Skamarock et al., 2008; Skamarock & Klemp, 2008) significantly underestimated warm-season precipitation over the Southern Great Plains, regardless of the

convection-permitting or convection-parameterizing configurations (Sun et al., 2016). Such a dry bias was also discovered in previous climate downscaling conducted by the North American Regional Climate Change Assessment Program (NARCCAP) (Mearns et al., 2012) and other individual studies (Berg et al., 2013; Gao et al., 2017; Harris & Lin, 2014; Kim et al., 2013; Lee et al., 2007b; Ma et al., 2014; Tian et al., 2017), while warm-season wet bias in the Southern Great Plains was rarely reported (Bukovsky & Karoly, 2009). Authors of these studies speculated that the dry bias was related to unrealistically strong coupling of the convection to surface heating over the Rocky Mountains and an abnormally slow eastward propagation of convective systems (Klein et al., 2006; Lee et al., 2007b; Tripathi & Dominguez, 2013). The possible reasons will be further investigated in this study using a large set of sensitivity downscaling simulations with different physics parameterization schemes with and without interior nudging.

In addition, we compare our downscaling results with those of the NARCCAP, a coordinated international program to investigate regional climate variability over North America using multimodel dynamical downscaling at a spatial resolution of 50 km (Mearns et al., 2012). Six RCMs (including the WRF model with the Grell cumulus scheme, referred to as WRFG) participated in Phase I of NARCCAP to downscale regional climate from the Reanalysis 2 (R2) data of the National Centers for Environmental Prediction (NCEP) and U.S. Department of Energy (DOE) (Kanamitsu et al., 2002). The simulation of WRFG in Phase I of NARCCAP will be referred to as NARCCAP WRFG hereafter. The downscaled precipitation fields from NARCCAP have been examined and evaluated for several purposes. For example, a few studies examined regional heavy daily precipitation events (e.g., Wehner, 2013). In particular, Kawazoe and Gutowski (2013) studied very heavy daily precipitation for the upper Mississippi River region during winter. Other studies evaluated the ability of NARCCAP RCMs to reproduce other precipitation characteristics for specific regions or seasons, e.g., coastal California and upper Mississippi River basin in the cold season (Gutowski et al., 2010); Intermountain Region (Wang et al., 2009); Oregon's Willamette River basin (Halmstad et al., 2013); Canada and the northern part of United States (Mailhot et al., 2012); Colorado in summer (Alexander et al., 2013); and California during wintertime (Caldwell, 2010). None of these NARCCAP-based studies have specifically examined the downscaled precipitation over the Great Plains in detail, however. For our study, the NARCCAP WRFG-downscaled precipitation will serve as a reference for improving dynamical downscaling of precipitation over the Great Plains.

Regional climate information, particularly in terms of precipitation, is critical for hydrologic assessment and management of water resource and flood risk (García-Valdecasas Ojeda et al., 2017; Halmstad et al., 2013). Previously, Qiao et al. (2014) assessed the hydrological responses of the trans-state Oologah Lake watershed in Northeast Oklahoma and Southeast Kansas to downscaled climate from NARCCAP using hydrologic simulations with the Variable Infiltration Capacity (VIC) model (Liang et al., 1994, 1999). Given the biases of the NARCCAP-downscaled precipitation fields (Mearns et al., 2012), the corresponding hydrological assessment likely lacks robustness.

This study aims to achieve a better precipitation downscaling over the Great Plains than previous studies, in particular those of Sun et al. (2016) and NARCCAP WRFG, using WRF version 3.8.1 which contains both grid and spectral nudging capabilities. WRF simulations will be first conducted and examined for a single representative warm season, during which previous downscaling showed significant biases, in order to identify an optimal configuration and to obtain a possible solution for reducing model precipitation biases. The resulting configuration is then used to produce regional climate downscaling over the Great Plains for a historical period of 36 years (1980–2015) during which precipitation data are available for verification. The hydrologic response of the Oologah Lake watershed to the downscaled precipitation is compared with the response to the NARCCAP WRFG-downscaled precipitation which has been previously assessed in Qiao et al. (2014).

The rest of this paper is organized as follows. Section 2 discusses the data, the simulation models, and configurations of the downscaling simulations. Section 3 discusses the downscaling results. Conclusions and further discussions (e.g., hydrologic applications of the downscaling outputs) are given in section 4.

2. Data and Methods

2.1. Precipitation Observations

The Stage IV precipitation data (Lin, 2011) have been archived continuously since January 2002, and they are available via http://data.eol.ucar.edu/codiac/dss/id=21.093. The precipitation data have a consistent

analysis record length of 15 years, and have high temporal and spatial resolutions that are valuable to this study (Herman & Schumacher, 2016). The Stage IV data combine the mosaicked hourly/6 hourly multisensor (i.e., radars and gauges) precipitation analyses (called Stage III) produced by the 12 River Forecast Centers of the National Weather Service. The data cover the contiguous United States (CONUS) and have a grid spacing of 4 km. The products are available for hourly, 6 hourly, and daily intervals. Stage IV data display an overall agreement with surface observations, although the products have a tendency to underestimate both annual and seasonal means as compared to surface observations (Nelson et al., 2016).

To make up the deficiency of relatively short record (15 years) of the Stage IV data, the Parameter-elevation Regressions on Independent Slopes Model (PRISM) precipitation data set (Daly et al., 1994) is

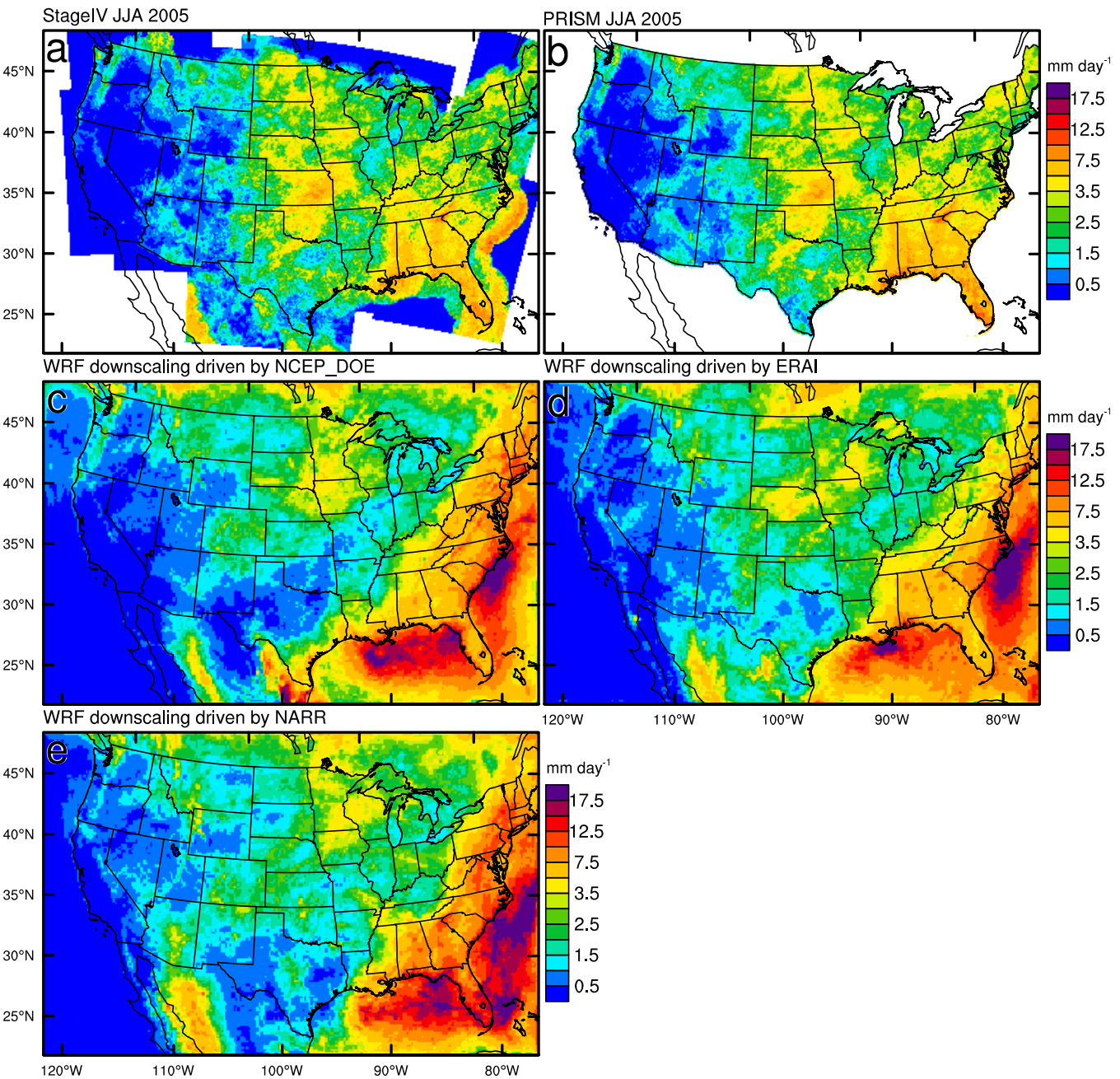

Figure 2. Mean precipitation rate in JJA 2005 retrieved from (a) the Stage IV, (b) PRISM data, and dynamically downscaled with WRF from the (c) NCEP/DOE R2, (d) ERA-interim, and (e) NARR reanalysis data.

selected for a longer-term model evaluation. PRISM produces monthly and annual average precipitation since 1895 (downloaded from http://www.prism.oregonstate.edu/) on regularly spaced grid cells over the CONUS domain at various spatial resolutions (800 m–4 km) based on point measurements and a digital elevation model (Prat & Nelson, 2015). We use the 4 km resolution monthly PRISM precipitation data in this study. Stage IV and PRISM data show similar spatial distributions of precipitation (e.g., Figures 2a versus 2b).

2.2. Study Periods

Our previous study (Sun et al., 2016) and the NARCCAP regional climate simulations (Mearns et al., 2012) significantly underestimated warm-season precipitation over the Great Plains, corroborating the generally accepted conclusion that accurate downscaling of summer precipitation in this region remains a great challenge for most RCMs (Leung & Gao, 2016; Liang et al., 2006; Wang & Kotamarthi, 2014; Qiao & Liang, 2015). Thus, to attain our goal of improving precipitation simulations over the Great Plains, we first focus on a single summer season (June, July, and August, i.e., JJA). We chose summer 2005 because it had sufficient rainfall to compare with simulations; in fact, the summer of 2005 was much wetter over the Great Plains than spring or fall of 2005 (Ramsey et al., 2014). A band of maximum precipitation over the Great Plains in JJA 2005 extended from north Texas northward to Kansas, where it peaked (Figure 2a). Previous downscaling for this period conducted by Wang and Kotamarthi (2014) also showed significant dry bias over the Great Plains.

To investigate the possible model errors responsible for the bias in downscaled precipitation, we conduct a nearly exhaustive set of sensitivity experiments for the month of August 2005 using different combinations of physics schemes available within WRF. After we have identified the model configuration with the least precipitation bias for the Great Plains, we use it to dynamically downscale the NCEP/DOE R2 data (Kanamitsu et al., 2002) for a 36 year period (1980–2015). This period is selected to encompass the 25 year time span (1980–2004) of the NARCCAP experiments as well as more recent years. In these multiyear downscaling simulations, the model is reinitialized every year following the approach of Wang and Kotamarthi (2014), but allowing for one extra month of spin-up, i.e., the model starts from 1 December of the previous year, runs for 13 months, and the outputs of the last 12 months are used for analysis. This reinitialization procedure allows for parallel executions of simulations for different years, improving the overall computational efficiency and turn around time on large parallel computers. We have compared results of reinitialized simulations with simulations continued from the end of the previous year; the differences are minimal as long as the spectral nudging is turned on because of the apparent lack of the initial condition memory beyond 1 month, in these simulations that are primarily forced at the lateral boundaries and interiorly nudged to the reanalysis data for long waves.

2.3. Three-Dimensional WRF Simulations

The WRF model has been used in a number of regional climate studies at various horizontal resolutions, including 12–50 km grid spacings (Bukovsky & Karoly, 2009; Caldwell et al., 2009; Leung et al., 2006; Lo et al., 2008; Wang & Kotamarthi, 2014; Wi et al., 2012; Zhang et al., 2009). Recently, it has been applied at the convection-permitting, 4 km grid spacing over large regions (Gao et al., 2012; Lee et al., 2017; Prein et al., 2017; Sun et al., 2016; Tian et al., 2017). However, such long-term, high-resolution simulations over large domains are computational very expensive and are not necessarily free of biases (Qiao & Liang, 2015; Sun et al., 2016); in fact, the 4 km WRF simulations reported in Sun et al. (2016) share similar precipitation biases as coarser resolution simulations that we have produced (not shown). For these reasons, we apply in this study WRF version 3.8.1 at a 20 km grid spacing and use it to downscale from the NCEP/DOE R2 data over the CONUS domain (see Figure 1b). The model domain has 44 vertical layers extending from the surface to 100 hPa. Table 1 summarizes the control configuration for WRF, which includes the Dudhia shortwave radiation scheme (Dudhia, 1989), the rapid radiative transfer model (RRTM) (Mlawer et al., 1997) for longwave radiation, the NOAH land surface model (Chen & Dudhia, 2001),

Table 1
Summary of the Control Model Configuration

Version	WRFv3.8.1 ARW
Short wave radiation	Dudhia
Long wave radiation	Rapid radiative transfer model (RRTM)
Boundary layer	YSU
Microphysics	Morrison
Cumulus	Grell-Freitas
Land surface model	NOAH
Vertical levels	44
Horizontal resolution	20 km × 20 km with 166 × 249 grid points
Time step	45 s
Initial and lateral boundary conditions	NCEP/DOE Reanalysis 2 (R2)
Interior nudging	None

Table 2
Summary of Physics Schemes Tested in the Sensitivity Downscaling for Summer 2005

Physics schemes	Abbreviations	Option number in WRF	Scheme names	References
Cumulus schemes	CU1	1	Kain-Fritsch (KF)	Kain (2004)
	CU2	2	Betts-Miller-Janjic (BMJ)	Janjic (1994)
	CU3 (control)	3	Grell-Freitas	Grell and Freitas (2014)
	CU4	4	Old Simplified Arakawa-Schubert (SAS)	Pan and Wu (1995)
	CU5	5	Grell-3	Grell and Devenyi (2002)
	CU6	6	Tiedtke	Tiedtke (1989) and Zhang et al. (2011)
	CU11	11	Multiscale KF	Zheng et al. (2016)
	CU14	14	New SAS	Han and Pan (2011)
PBL schemes	PBL1 (control)	1	YSU	Hong et al. (2006)
	PBL7	7	ACM2	Pleim (2007)
	PBL8	8	BouLac	Bougeault and Lacarrere (1989)
Microphysics schemes	MP1	1	Kessler	Kessler (1969)
	MP6	6	WSM6	Hong et al. (2004)
	MP10 (control)	10	Morrison 2-mom	Morrison et al. (2009)
Land surface models	LS2 (control)	2	NOAH	Chen and Dudhia (2001)
	LS3	3	RUC	Smirnova et al. (2000)

Note. For each sensitivity simulation, only a specific scheme is changed, but the rest configurations are the same as the control configuration summarized in Table 1. Note that only selected ones shown in figures are listed.

the Yonsei University (YSU) boundary layer scheme (Hong et al., 2006), the Grell-Freitas cumulus scheme (Grell & Freitas, 2014), and the Morrison microphysics scheme (Morrison et al., 2009). No interior nudging is applied in the control configuration.

Based on the control simulation, we conduct sensitivity experiments with 9 cumulus, 20 microphysics, 2 land surface, and 7 boundary layer schemes (total $9 + 20 + 2 + 7 = 38$ experiments) for summer 2005. These physics parameterization schemes have been shown to markedly affect downscaled precipitation output in previous studies (Klein et al., 2015). The full list and description of the parameterization schemes can be found at http://www2.mmm.ucar.edu/wrf/users/docs/user_guide_V3.8/users_guide_chap5.htm#summary, and Table 2 lists those whose results are shown in this manuscript. To ensure that the forcing data does not affect our results significantly, we also conduct sensitivity simulations for summer 2005 using two other reanalysis data sets, i.e., the North American Regional Reanalysis (NARR) (Mesinger et al., 2006) and the ERA-interim data (European Centre for Medium-Range Weather Forecasts, 2009). Most importantly, we examine the impact of applying interior nudging through experiments with and without nudging.

3. Results

3.1. Improvement of Precipitation Downscaling in Summer 2005

Our previous 10 year dynamic downscaling significantly underestimates warm-season precipitation over the Great Plains (Sun et al., 2016). The same issue also occurs with NARCCAP 25 year downscaling, particularly with the WRFG member (Mearns et al., 2012). To diagnose the issue, we first perform WRF simulations using NCEP/DOE R2 for JJA 2005. Similar to Sun et al. (2016), the WRF model with the control configuration (Table 1) again significantly underestimates the precipitation over the Great Plain area (by −49.7%, Table 3), especially over Kansas and Oklahoma (Figure 2c), even though the configuration of this study is different from that used in Sun et al. (2016). Results for the single month of August 2005 (Figure 3b) are similar to that of JJA. Because regional WRF simulations have been shown to be sensitive to the uncertainties in the large-scale forcing (Michelson & Bao, 2008), we also used two other reanalysis data sets (i.e., ERA-interim and NARR) to drive the WRF downscaling. Although sensitivities of the downscaling results to the reanalysis data sets are found, the spatial distribution of the downscaled precipitation is not improved with the use of different reanalysis forcing (Figure 2). With NARR, the Great Plains appear even drier (underestimated by

Table 3
Statistics for the Downscaled 2005 JJA Mean Precipitation Rate Over the Great Plains Area Marked in Figure 1 for Simulations Shown in Figures 2 and 5

	Mean precipitation rate (mm d^{-1})	Normalized mean bias (NMB) relative to Stage IV (%)		Mean precipitation rate (mm d^{-1})	Normalized mean bias, NMB (%)
Below are for observations and simulations without spectral nudging shown in Figure 2					
Stage IV	4.0		PRISM	3.9	
driven by NCEP/DOE R2	2.0	−49.7	Driven by ERA-Interim	2.5	−36.7
driven by NARR	1.9	−52.0			
Below are for simulations with spectral nudging shown in Figure 5					
ACM2 (PBL7)	4.3	6.7	BMJ (CU2)	2.4	−39.5
Grell-Freitas (CU3)	3.7	−6.8	Grell-3 (CU5)	4.1	2.0
KF (CU1)	4.1	3.1	Multiscale KF (CU11)	3.6	−9.7
Tiedtke (CU6)	3.1	−22.6	New SAS (CU14)	2.8	−29.2

−52%, Table 3), with the precipitation over Nebraska significantly reduced. These simulations indicate that the dry bias over the Great Plains seen in previous studies is not caused by a particular reanalysis product. In addition, a similar dry bias in the Great Plains has also been reported from simulations using other regional climate models (Berg et al., 2013; Harris & Lin, 2014; Lee et al., 2007b; Ma et al., 2014) and speculated to be related to unrealistically strong coupling of convective processes to the surface heating over the

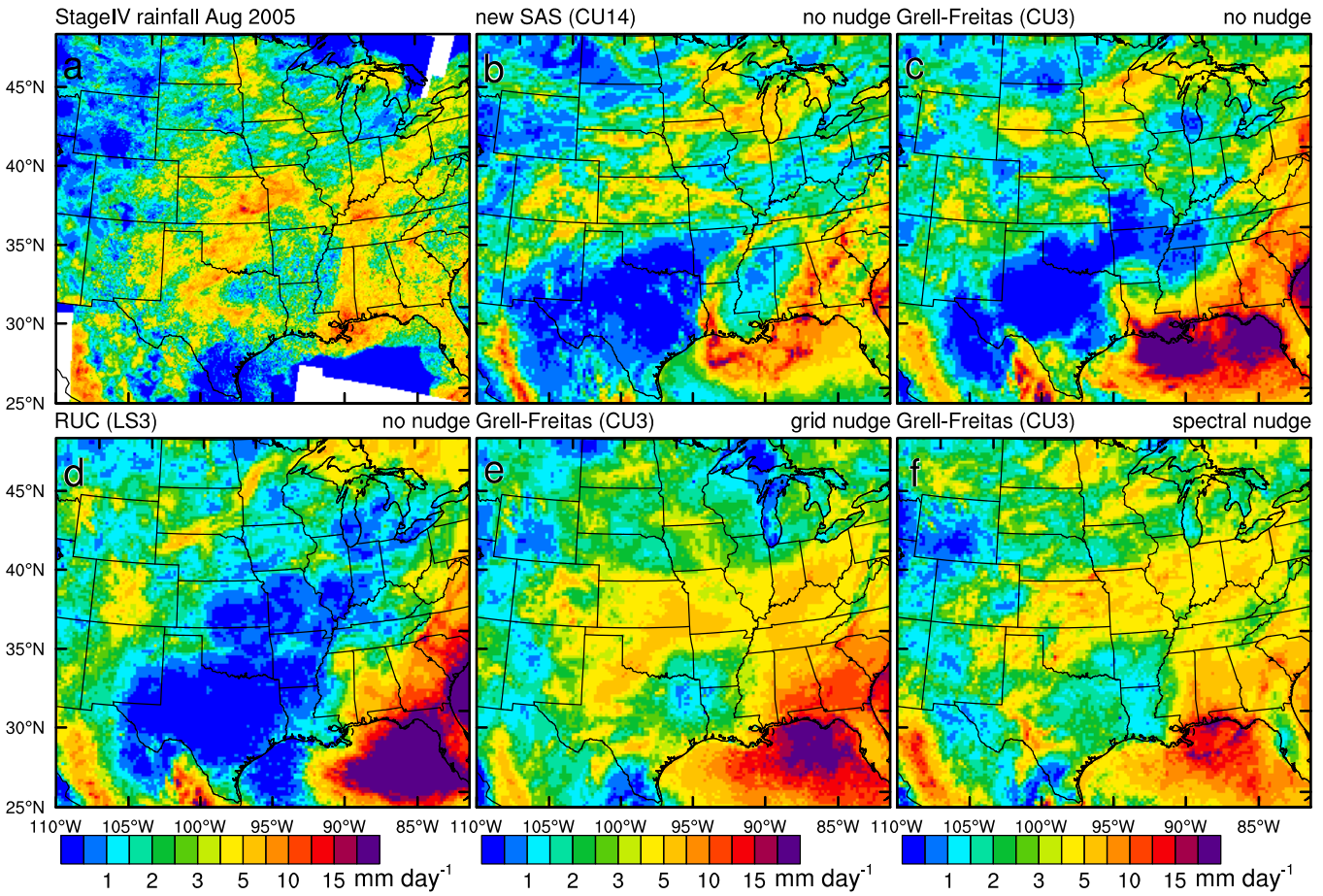

Figure 3. Mean precipitation rate in August 2005 retrieved from (a) the Stage IV data and dynamically downscaled with WRF (b, c, d) with different physics schemes but no nudging, (e) with grid nudging, and (f) with spectral nudging. See the explanation of abbreviations of physics parameterization schemes in Table 2.

Rocky Mountains and to abnormally slow eastward propagation of convective systems (Klein et al., 2006; Lee et al., 2007b; Tripathi & Dominguez, 2013).

To investigate if certain model physics parameterizations can alleviate the warm-season dry bias over the Great Plains, we ran a large set of sensitivity simulations with 9 cumulus schemes, 2 land surface models, 7 PBL schemes, and 20 microphysics schemes for a representative month (i.e., August 2005) when WRF simulations suffer severe dry bias over the southern Great Plains. Unfortunately, all of these simulations show similar biases in terms of precipitation location (results from three sensitivity simulations are shown in Figures 3b–3d); that is, precipitation in Kansas, Oklahoma, and Texas is underestimated (similar as the JJA mean shown in Figure 2) and precipitation in the Rockies is overestimated, thus shifting the southern Great Plains rain band northwestward, as is also reported in Sun et al. (2016) (see their Figure 2).

Over the past several years, the Center for Analysis and Prediction of Storms at the University of Oklahoma has been carrying out real-time numerical weather prediction (NWP) using the WRF model, with a focus on precipitation and severe weather (Kong et al., 2011; Xue et al., 2007, 2009, 2010). In these real-time forecasts up to several days, systematic bias in precipitation location around the Great Plains does not occur. Thus, we suspect that the bias in the regional climate simulations is rooted in the downscaling framework. The core differences between NWP and climate downscaling include: (1) different driving data (i.e., forecast data for NWP versus reanalysis data for downscaling of the historical period) and (2) different initialization strategies (i.e., daily reinitialization for short-term NWP versus a single initialization for continuous, long-range simulations). However, reanalysis data should be generally more accurate than the forecast data used at the lateral boundaries because of all the observations assimilated into the reanalysis fields. In addition, our simulations driven by different reanalysis data sets (Figure 2) share similar precipitation biases. Thus, it is unlikely that systematic biases in the driving reanalysis data caused the precipitation biases.

Given the above discussions, we speculate that error accumulation within the long regional climate simulations is an important cause for the systematic precipitation bias. To assess this speculation, instead of initializing once and running the simulation for a full month of August, we reinitialize the simulations on a daily basis (similar to the NWP runs). When the simulations are reinitialized daily, the southern Great Plains rain band is indeed much better reproduced, particularly in terms of its location (figure not shown). The sensitivity to the initialization strategies indicates that model bias accumulated through the continuous (monthly, seasonally, or longer) climate simulations does appear to be a key reason for the simulated precipitation biases. For regional climate simulations, daily reinitialization from reanalysis is clearly not an acceptable strategy. Ideally, the true source of model error causing the error accumulation is uncovered and an improvement to the model is implemented to reduce the error. Unfortunately, our exhaustive testing with different combination of model physics parameterizations did not give us much of a clue; finding a fix to the simulation model has to be left for further studies.

In the absence of a true fix to the model bias, one possible solution to prevent the systematic solution drift is to nudge the large-scale fields within the simulation domain toward the external forcing. Interior nudging had proven successful previously in dynamical downscaling of regional climate (Hu et al., 2017; Huang et al., 2016; Mabuchi et al., 2002; Miguez-Macho et al., 2004; Lo et al., 2008; Liu et al., 2012; Paul et al., 2016; Prein et al., 2017; Spero et al., 2014; von Storch et al., 2000). WRF supports two forms of interior nudging: analysis nudging (also called "grid nudging") and spectral nudging (Miguez-Macho et al., 2004, 2005; Wang & Kotamarthi, 2013). Analysis nudging adjusts simulations toward the driving fields (from the reanalysis or the GCM simulations) regardless of the scales of motion (thus also called indiscriminate nudging or nonscale-selective nudging) through adding a nonphysical term to the model equation:

$$\frac{dQ}{dt} = L(Q) - K(Q - Q_o) \tag{1}$$

where Q is any of the prognostic variables to be nudged, Q_o is the corresponding variable from the driving fields, L is the model physical forcing term (including advection, Coriolis effects, etc.), and K is the nudging coefficient, whose inverse is the e-folding time scale. In contrast, spectral nudging forces *only the long wavelengths* of nudged variables toward the driving fields (Miguez-Macho et al., 2004) through

Table 4
Summary of Spectral Nudging Configurations

Nudging variables	Horizontal wind components, temperature, geopotential height
Nudging coefficient	3×10^{-5} s^{-1}
Nudging height	Above PBL
Wave number	5 and 3 in the zonal and meridional directions, respectively
Nudging period	Throughout the downscaling simulation

$$\frac{dQ}{dt} = L(Q) - \sum_{|n|\le N} \sum_{|m|\le M} K \cdot (Q_{mn} - Q_{omn}) e^{ik_m x} e^{ik_n y}, \quad (2)$$

where m and n are the number of waves in the x and y directions, respectively, across the model domain, Q_{mn} and Q_{omn} are the spectral coefficients of Q and Q_o respectively. k_m and k_n are the wave vector components in the x and y directions, which are expressed in terms of discrete wave numbers m and n and domain size D_x and D_y:

$$k_m = \frac{2\pi \cdot m}{D_x};\ k_n = \frac{2\pi \cdot n}{D_y}. \quad (3)$$

Because the primary purpose of regional climate downscaling is to produce more smaller scale details not present in the driving large-scale fields while trying to maintain a consistency between the downscale solutions and the driving fields at the large scales, spectral nudging is a reasonable choice for the downscaling purpose. Hence, we apply the spectral nudging configurations (including nudging variables, nudging strength, nudging height, wave number; Table 4) suggested by Wang and Kotamarthi (2014) for their WRF-based downscaling. Particularly we adopted nudging wave numbers of 5 and 3 in the zonal and meridional directions over CONUS, thus nudging long waves with wavelengths of ~1,000 km to those of the driving fields. The suggested nudging coefficient of 3×10^{-5} s^{-1} is adopted, which corresponds to a ~9 h time scale. Stronger nudging with larger nudging coefficients on more wave numbers was shown to have a detrimental effect on downscaled precipitation over the Great Plains, particularly on the detailed structures of precipitation, since it may destroy the mesoscale features simulated by the dynamic model (Tian et al., 2017; Wang & Kotamarthi, 2014). Gomez and Miguez-Macho (2017) explicitly suggest that 1,000 km is the optimal scale threshold to nudge in order to balance the constraint from the driving fields and fine-scale contribution from the downscaling model.

Still, to examine the impacts of nudging over all wavenumbers, we also performed downscaling experiments with grid nudging. With either form of nudging, the simulated rain band location in the southern Great Plains during August 2005 is significantly improved (Figures 3e and 3f). The model simulates more precipitation in Texas, Oklahoma, Kansas, and Missouri with either nudging than without, leading to a better agreement with the Stage IV data (Figure 3a).

Comparing to the spectral nudging, the grid nudging simulates wider spread precipitation with gentler spatial variations. A spectral analysis of the observed and downscaled precipitation fields using the Discrete Cosine Transform (DCT; Denis et al., 2002) is conducted to further illustrate the difference in the effects of two forms of nudging. DCT is preferred over the Fourier transform for analyzing two-dimensional (2-D) atmospheric fields over limited-area domains and it was previously used to evaluate precipitation forecasts (Surcel et al., 2014). 2-D DCT spectral variances are computed for observed (i.e., Stage IV) and downscaled daily precipitation fields during August 2005 within a square domain over the Great Plains. This square domain (Figure 4e) is selected for three reasons: (1) precipitation variation over the Great Plains is the focus of this study, (2) the domain needs to be within the coverage of the Stage IV data in order to compute the spectra of Stage IV observations, and (3) DCT analysis over a square domain is simpler and easier to interpret than that over a rectangle domain. The mean 2-D spectral variance and the binned 1-D power spectra during this month are shown in Figure 4. Both grid nudging and spectral nudging underestimate the variance of daily precipitation over short waves (with wavelength <600 km) and the underestimation by grid nudging is more severe. The difference seen in Figure 4 between grid nudging and spectral nudging can be explained by equations (1) and (2). Grid nudging adjusts nudged variables toward the driving fields (i.e., the R2 reanalysis) regardless of the scales of motions. Thus, the scale of motion resolved by the grid nudging is close to the R2 reanalysis (with a 2.5° grid spacing), for which the smallest resolvable wavelength in DCT algorithm is ~500 km (2 grid spacing). Consequently, the smaller scale motion is damped during the grid nudging process. In contrast, spectral nudging only forces the long waves (with wavenumber ≤5 and 3 in zonal and meridional directions over the simulation domain, roughly wavelength >1,000 km) of nudged variables to the driving fields and allow the model dynamics to develop small-scale motions. Thus, the smallest resolvable wavelength in the DCT algorithm by the spectral nudging is 2 times model grid spacing, i.e., 40 km. As a result, the power spectra for short waves (<500 km) of nudged variables are less

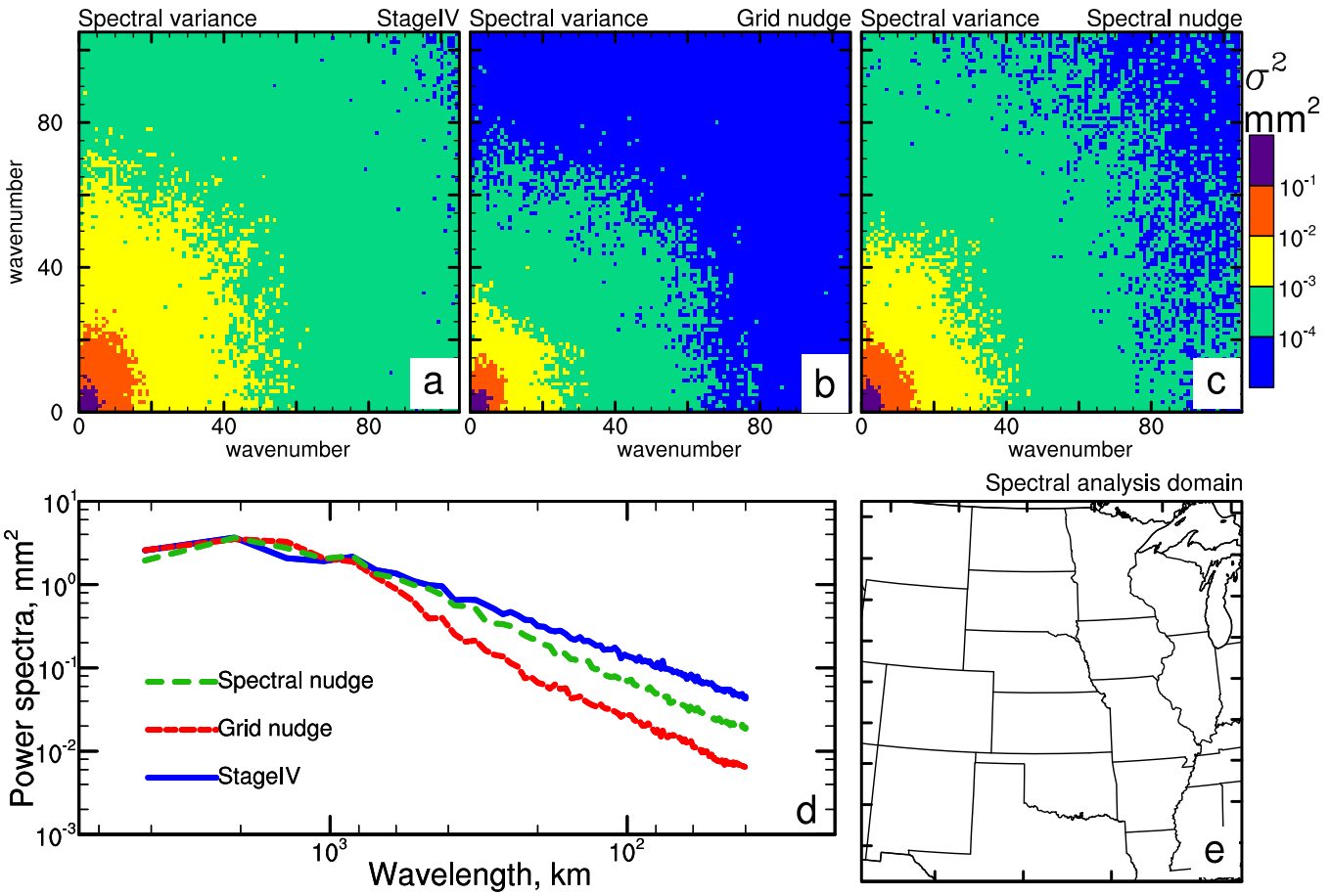

Figure 4. Two-dimensional (2-D) mean spectral variance of daily rainfall fields during August 2005 from (a) Stage IV, (b) WRF downscaling with grid nudging, (c) WRF downscaling with spectral nudging computed using the Discrete Cosine Transform (DCT) over the selected domain shown in plot (e). The 2-D spectrum is binned according to the equivalent wavenumbers to produce (d) the power spectra solely as a function of equivalent wavenumber (but not direction). Note that the Stage IV has a higher resolution (~4 km) than WRF (20 km), thus can resolve more high frequency waves than WRF. But to compare with WRF, the larger wavenumbers resolved by Stage IV are not shown in plots a and d.

underestimated by spectral nudging than grid nudging, as also previously reported (e.g., Gomez & Miguez-Macho, 2017; Otte et al., 2012; Vincent & Hahmann, 2015). Precipitation, an unnudged variable, responds to the nudged variables and also shows significant underestimation by grid nudging at scales with wavelength $<$500 km (Figure 4d). The spectral analysis thus further corroborates that spectral nudging is superior than grid nudging for dynamic downscaling.

Given the superiority over the downscaling without nudging or with grid nudging, spectral nudging is also applied in the downscaling of JJA 2005. Much better precipitation simulation is again obtained with spectral nudging for these months over the southern Great Plains (Figure 5a) than without (Figure 2c), as compared to the Stage IV data set (Figure 2a).

The benefit of spectral nudging lies in its ability to constrain the large-scale circulation patterns in the regional domain to match those of external forcing. For example, Figure 6 shows the deviations of the simulated JJA mean circulation and geopotential height fields from those of NCEP R2 with and without spectral nudging. Relative to the driving NCEP R2 reanalysis, an anomalous anticyclonic circulation develops in the simulation without spectral nudging over the southern Great Plains and southwest U.S. while an anomalous cyclonic circulation occupies the eastern coastal region (Figure 6a). The northerly wind anomaly in the eastern flank of the anticyclonic circulation anomaly effectively decreases the prevailing southerly flows over the Great Plains along the western edge of the Bermuda High (Figure 7). Climatologically, these prevailing southerlies bring moisture from the Gulf of Mexico to the Great Plains (Arritt et al., 1997; Gomez & Miguez-Macho, 2017; Higgins et al., 1997). Thus, the anticyclonic circulation anomaly that develops in the simulation

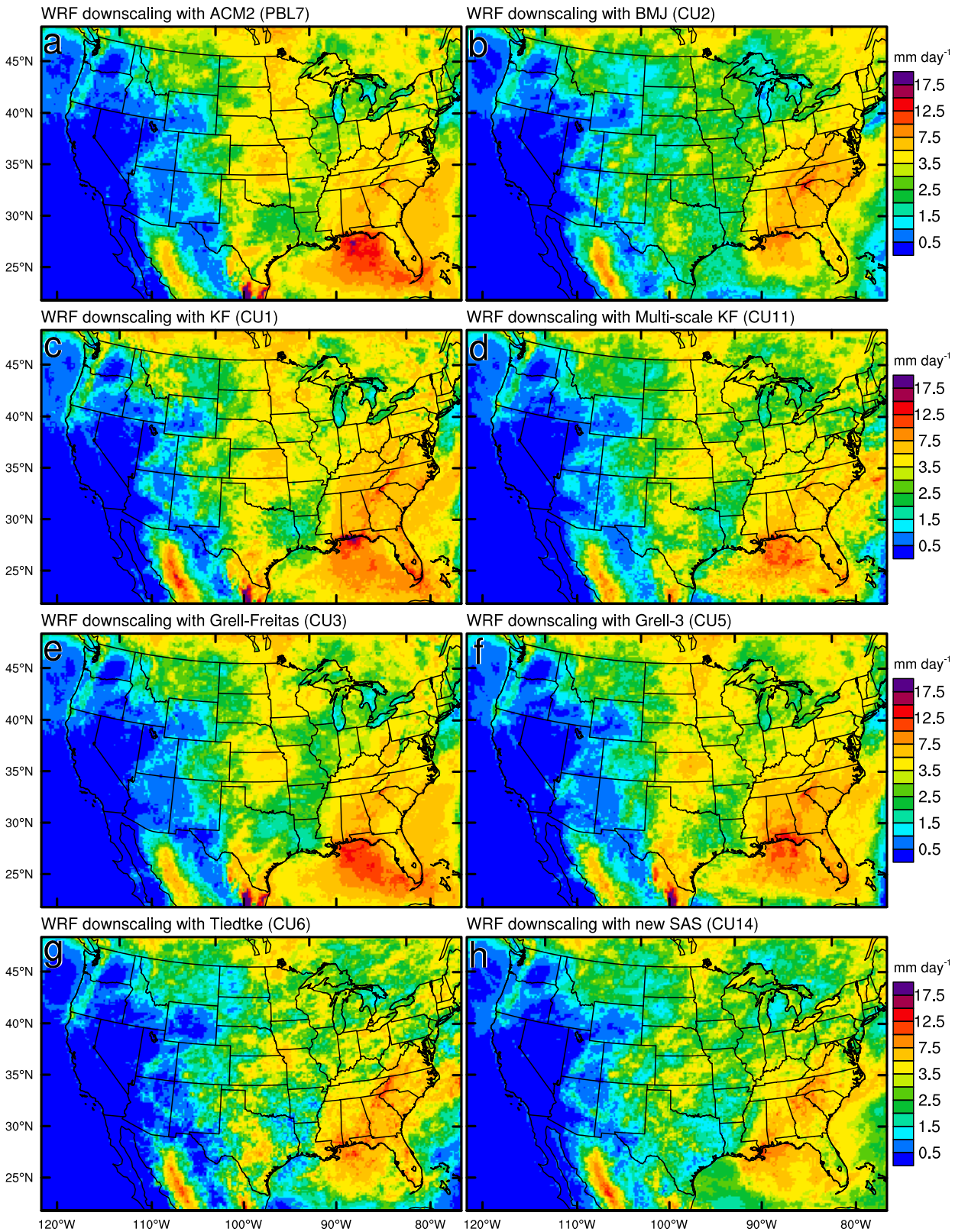

Figure 5. Mean precipitation rate in JJA 2005 dynamically downscaled with WRF with spectral nudging and with (a) the ACM2 PBL scheme and with different cumulus schemes, i.e., (b) BMJ (CU2), (c) KF (CU1), (d) multiscale KF (CU11), (e) Grell-Freitas (CU3), (f) Grell-3 (CU5), (g) Tiedtke (CU6), and (h) new SAS (CU14). The corresponding observations are shown in Figures 2a and 2b.

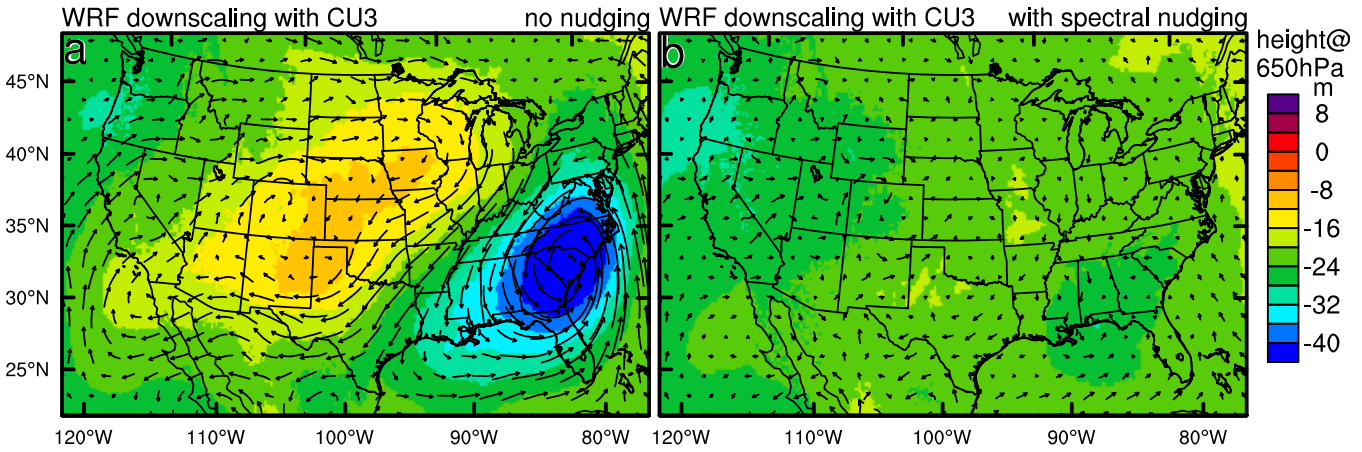

Figure 6. Geopotential height difference during JJA 2005 between WRF downscaling and NCEP/DOE R2, (a) without and (b) with spectral nudge.

without spectral nudging results in a decreased moisture supply (Figure 7) and therefore suppressed precipitation over the southern Great Plains. Meanwhile, the cyclonic circulation anomaly over the Southeast U.S. leads to excessive precipitation over the region (Figure 2c). Spectral nudging successfully eliminates those spurious circulation anomalies (Figure 6b), leading to a spatial distribution of precipitation (Figure 5a) much closer to that observed (Figure 2a).

Note that the downscaled WRF simulations have systematically lower geopotential heights than NCEP/DOE R2 fields by about 20 m across the whole domain (Figure 6). This bias may be due to different vertical coordinate systems between WRF and NCEP/DOE R2. There are also some noisy differences of geopotential height between WRF and NCEP/DOE R2 along the boundary where mountains reside. Note that terrain heights used in WRF are interpolated by the WRF Preprocessing System (WPS), which differ from that of the modeling system used to produce the reanalysis data; such differences are more pronounced in mountainous regions (Gochis et al., 2003).

3.2. Impact of Different Physics Schemes

3.2.1. Impact on Precipitation Amount

With the large-scale circulations more accurately simulated by applying spectral nudging, the sensitivity of regional climate downscaling to different physics schemes can be examined in a more meaningful way. With spectral nudging always turned on, we run the JJA 2005 simulations with different physics parameterizations (see Table 2 for those selected to show in Figures 3 and 5). To show only the most important similarities and differences, Figure 5 highlights results from representative simulations for each

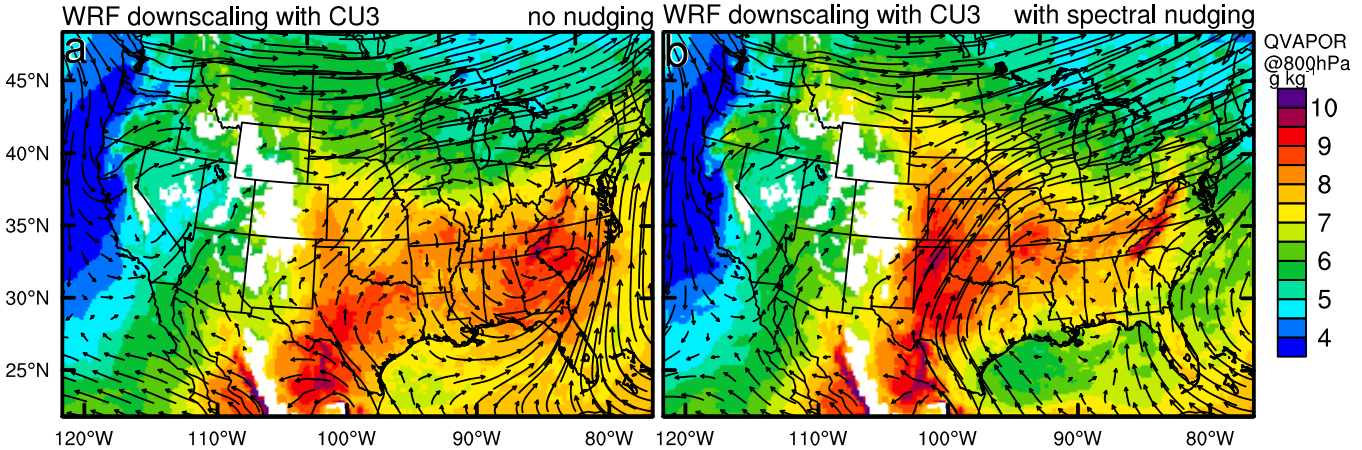

Figure 7. Downscaled water vapor mixing ratio (QVAPOR) and wind fields at 800 hPa during JJA 2005 (a) without and (b) with spectral nudge.

parameterization category (e.g., PBL) or simulations with prominent differences from the base simulation. Different cumulus schemes are found to lead to more pronounced differences than other physics schemes tested in terms of precipitation amounts over the Great Plains. Previous studies (e.g., Argueso et al., 2011; Flaounas et al., 2011; Jankov et al., 2005; Lynn et al., 2009; Sikder & Hossain, 2016; Zhang et al., 2011) at non-convection-permitting/resolving resolutions have also found stronger sensitivity of simulated cloud and precipitation to cumulus schemes than to other physics schemes such as the PBL, microphysics schemes. In particular, the BMJ (CU2), new SAS (CU14), and Tiedtke (CU6) schemes simulate substantially lower precipitation over the Great Plains than other cumulus schemes (Figure 5 and Table 3), which is consistent with Qiao and Liang (2015). It was speculated that cumulus schemes originally developed and often used in coarse-resolution GCMs (e.g., Tiedtke in the ECMWF global model, new SAS in the NCEP's Global Forecast System) are more likely to systematically underestimate the summer rainfall amount over the Great Plains (Qiao & Liang, 2015). Recent modifications to the convective cloud-base mass flux, convective inhibition, and convective detrainment processes in the new SAS, some addressing scale dependency (scale awareness), were reported to lead to stronger precipitation and better-organized precipitation patterns, thus can potentially improve precipitation simulation (Kwon & Hong, 2017; Lim et al., 2014).

The underestimated precipitation rate and widespread precipitation area produced by the BMJ scheme (Figure 5b) agree with the well-known characteristic of the scheme. The BMJ scheme uses a profile-relaxation approach to adjust the simulated sounding toward a postconvective reference profile (Betts, 1986; Betts & Miller, 1986; Janjic, 1994). BMJ was previously reported to often lead to a too dry conditions (Gochis et al., 2002; Jankov et al., 2005) and generate large areas of light rainfall while severely underestimate summertime precipitation rates over U.S. (Gallus, 1999) and Europe (Pieri et al., 2015).

Multiscale KF (CU11) leads to lower precipitation (3.6 mm d^{-1}, with NMB of −9.7%) over the Great Plains than the KF (CU1) scheme (4.14 mm d^{-1}, with NMB of 3.1%, Table 3), which is consistent with the original design of the multiscale KF scheme to reduce the excessive precipitation sometimes presented in weather forecasts with the KF scheme (Zheng et al., 2016). The KF scheme uses a mass flux approach to rearrange mass in an atmosphere column to remove at least 90% of the convective available potential energy (CAPE) (Kain, 2004). Unlike the BMJ scheme that is primarily driven by the thermodynamics of the simulated sounding, thus is not directly impacted by vertical motion, the KF scheme is more influenced by surface convergence and the resulting vertical motion (Gallus, 1999). Thus, KF can be more easily activated than the BMJ scheme and consequently leads to more precipitation than BMJ (Gochis et al., 2002). Also KF may produce unrealistically deep saturated layers in postconvective sounding, which can lead to postconvective stratiform precipitation and overprediction of total precipitation (Pieri et al., 2015). To mitigate the precipitation overprediction, Zheng et al. (2016) together with Herwehe et al. (2014) designed the multiscale KF scheme by introducing a few changes to the KF scheme, including subgrid-scale cloud-radiation interactions, a dynamic adjustment time scale, impacts of cloud updraft mass fluxes on grid-scale vertical velocity, and scale-dependent lifting condensation level-based entrainment. These changes appear to reduce precipitation as shown in Figures 5c and 5d.

Two variants of the Grell cumulus scheme (i.e., Grell-Freitas and Grell-3) are available in WRF, both of which are improved versions of a stochastic scheme originally implemented by Grell and Devenyi (2002). The Grell-3 (CU5) scheme spreads subsidence on neighboring grid points while the Grell-Freitas (CU3) scheme is based on a scale-aware method recently introduced by Arakawa et al. (2011). The Grell-Freitas (CU3) scheme leads to lower precipitation (3.7 mm d^{-1}, with NMB of −6.8%) over the Great Plains than the Grell-3 (CU5) scheme (4.1 mm d^{-1}, with NMB of 2.0%, Table 3), which is different from the sensitivity over Brazil, where Grell-Freitas produced slightly (barely discernable) more precipitation than Grell-3 (Grell & Freitas, 2014). The different sensitivity to Grell-Freitas and Grell-3 in different regions may be due to the different characteristics of precipitation. Note that the simulations are conducted at a 20 km horizontal grid spacing in this study. The benefit of the scale-aware Grell-Freitas scheme may be more appreciable when applied to gray-zone resolutions (defined as 1–10 km in Kwon and Hong (2017), 4–10 km in Prein et al. (2015), and 4–15 km in Gao et al. (2017)) where the assumption of conventional cumulus schemes (that is, convective clouds cover only a small fraction of the model grid cell) starts to break down but moist convections are not completed resolved yet (Fowler et al., 2016). Note that the gray zone here is framed from the perspective of cloud microphysics, which is different from the gray zone defined from the perspective of turbulence (Bryan et al., 2003; Shin & Hong, 2015; Wyngaard, 2004; Zhou et al., 2017).

Different PBL schemes simulate different PBL thermodynamic and kinematic properties, which can cause differences in precipitation. In this case, however, altering PBL schemes does not lead to significant change in the precipitation amount (Figure 5a). The relationship between PBL properties and subsequent precipitation is complicated (Klein et al., 2015; Trier et al., 2008), especially during the warm season in the Great Plains, where the precipitation may be influenced by mesoscale vertical circulation, eastward propagating convection, and large-scale moisture advection (Dai et al., 1999; Findell et al., 2011; Liang et al., 2006; Martynov et al., 2013; Qiao & Liang, 2015; Schumacher et al., 2013). In addition, some PBL schemes have different treatments for stable and unstable boundary layers (Hu et al., 2010a, 2013) and thus have different performances for different time of day, which further complicates the identification of the effect of different PBL schemes on precipitation.

One key aspect of PBL schemes is their vertical mixing strength (Hu et al., 2010a) which can be dictated by a few important parameters in the schemes (Hu et al., 2012; Klein et al., 2016; Nielsen-Gammon et al., 2010). We chose to examine the sensitivity of a critical parameter in the YSU scheme that controls the daytime vertical mixing strength (p, an exponent affecting the magnitude and vertical distribution of eddy diffusivity within the PBL) identified by Hu et al. (2010b). Results show that larger values of p lead to weaker vertical mixing and lower PBL heights, consistent with the formulation of eddy diffusivity (Hu et al., 2010a). Consequently, lower PBL heights lead to more moisture near the surface and stronger CAPE in the afternoon. As a result, more precipitation is predicted in the afternoon, especially in the mountains and southeast U.S. (not shown). On the other hand, smaller values of p lead to higher PBL heights and consequently less precipitation. This sensitivity of simulated precipitation to different simulated PBL heights is consistent with the previous study of Trier et al. (2011).

Altering microphysics schemes does not change the precipitation amounts markedly, except that the Kessler scheme significantly underpredicts precipitation over most of the continent (figure not shown) likely due to its complete ignorance of important ice microphysical processes.

3.2.2. Impact on the Diurnal Variation of Precipitation

Single-minded pursuit of the "best" performance in terms of total precipitation over the Great Plains may not be encouraged because some configurations may simulate the right amount of total precipitation but at wrong time. As seen in Figure 1a, the precipitation across the Great Plains has unique diurnal and spatial variations, the precipitation peaks during nighttime and generally moves from west to east. Figure 8 shows the performance of 10 selected physics configurations in terms of the diurnal variation of precipitation over the Rockies and Great Plains (the exact areas are marked using two boxes in Figure 1a). Note that the hourly precipitation rate shown in Figure 8 is normalized by the daily mean value, as in Liang et al. (2004b). Over the Rockies, all schemes predict peak precipitation in the afternoon, spanning from 1400 to 1700 local time, while the Stage IV product shows peak precipitation at 1500 local time (Figure 8a). In contrast, the sensitivity of diurnal variation of precipitation to different parameterization schemes (particularly cumulus schemes) over the Great Plains is more pronounced (Figure 8b). Altering PBL and microphysics schemes does not change diurnal variation of precipitation significantly, while cumulus parameterization strongly affects the diurnal variation of precipitation. The Stage IV data show a prominent diurnal variation of precipitation over the Great Plains with daytime minimum and nighttime peak. The KF (CU1), BMJ (CU2), and Grell-3 (CU5) schemes erroneously place the peak precipitation over the Great Plains during the afternoon and miss the nighttime peak. The Grell-Freitas (CU3), new SAS (CU14), multiscale KF (CU11), and Tiedtke (CU6) capture the nighttime peak over the Great Plains. The behaviors of cumulus schemes are generally consistent with those seen in previous studies (Leung & Gao, 2016; Liang et al., 2004b, 2006).

In summary, all the cumulus schemes perform relatively well over the Rockies and perform markedly differently over the Great Plains in terms of reproducing the diurnal variation of precipitation. These different performances are related to the characteristics of precipitation in different regions. Over the Rockies, the precipitation is dictated by (and peaks the same time as) boundary layer thermodynamic forcing such as surface fluxes and thermodynamic properties of the near-surface air, while the precipitation over the Great Plains is more governed by large-scale dynamic forcing such as free tropospheric advection/convergence (Lee et al., 2007a; Zhang, 2003) and low-level jets (Harding et al., 2013). It appears all the cumulus schemes perform fine over regions where precipitation is governed by boundary layer thermodynamic forcing, e.g., the Rockies (Figure 8a) and the Southeast U.S. (figure not shown); while some cumulus schemes perform poorly over the Great Plains where peak precipitation is more in phase with large-scale forcing.

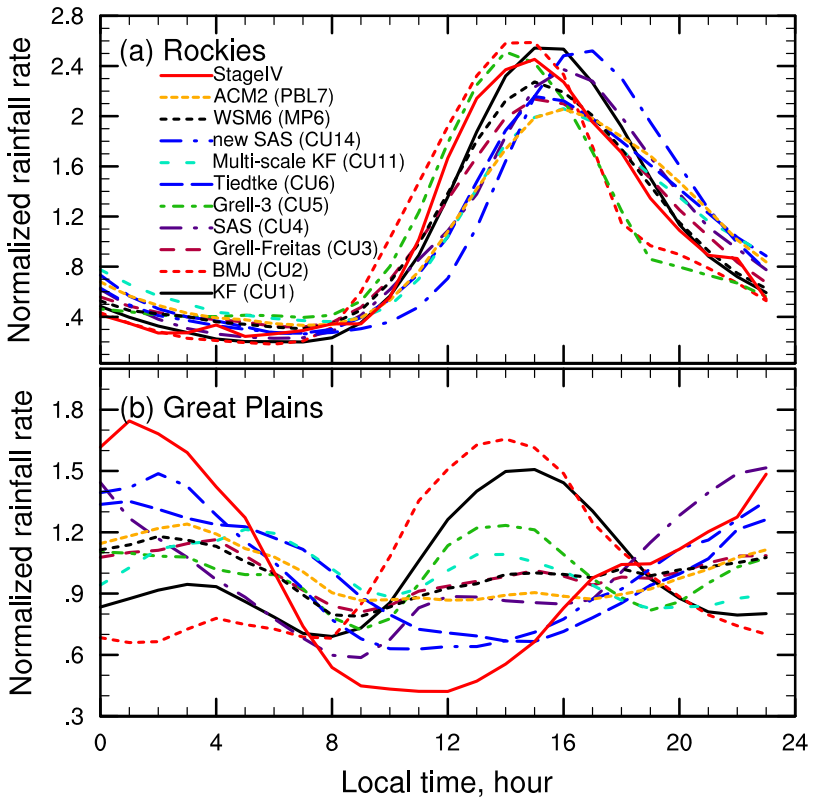

Figure 8. Diurnal variation of normalized rainfall rate during JJA 2005 over the (a) Rockies and (b) Great plains. The hourly precipitation rate is normalized by the daily mean value, as in Liang et al. (2004b).

The closure assumption and trigger function adopted in cumulus schemes were reported to play a key role in dictating diurnal variation of precipitation (Choi et al., 2015; Qiao & Liang, 2015; Xie & Zhang, 2000; Zhang, 2002, 2003). Those closure assumptions and trigger functions that couple moist convection too strongly with boundary layer thermodynamic forcing and too weakly with large-scale forcing are likely to fail to accurately predict the observed nocturnal precipitation maxima over the Great Plains (Liang et al., 2004b; Qiao & Liang, 2015; Xie & Zhang, 2000). For the two worst cumulus schemes in terms of simulated precipitation diurnal variation (i.e., KF and BMJ), a previous study (Qiao & Liang, 2015) has shown that the closure assumption of an instantaneous relaxation of thermodynamic profiles toward an quasi-equilibrium reference state, used in BMJ (Baldwin et al., 2002; Bukovsky et al., 2006; Janjic, 1994), and the assumption of CAPE being nearly completely removed by convection over a short time period (0.5–1 h), as in KF (Kain, 2004), are incapable of reproducing the correct timing of convection (i.e., the nighttime rainfall peak) in the Great Plains. Similar was also found by Clark et al. (2009) and Leung and Gao (2016) when comparing convection-allowing and convection-parameterized precipitation forecasts over the Great Plains.

For four other schemes that perform better in terms of diurnal variation of precipitation (i.e., Grell-Freitas (CU3), new SAS (CU14), multiscale KF (CU11), and Tiedtke (CU6)), the closure treatments are different. Grell-Freitas adopts a large-scale instability tendency closure, which is more sensitive to large-scale tropospheric forcing, in comparison to the KF scheme which is heavily influenced by the boundary layer forcing (Liang et al., 2004b). Thus, the Grell-Fritsch scheme performs better over the Great Plains where the diurnal timing of convection is influenced by the large-scale vertical motion (Dai et al., 1999). For the new SAS scheme, a comprehensive convection trigger function is used, which evaluates two conditions for convection initiation: (1) the cloud base (defined as the level of free convection) must be within 150 hPa depth from the convection starting level (defined as the level of maximum moist static energy) and (2) the cloud work function (CWF) exceeds a critical CWF calculated as a function of the large-scale vertical velocity at the cloud base. This comprehensive trigger function was found to play a key role in reproducing the diurnal variation of precipitation over the Great Plains (Lee et al., 2008; Wang et al., 2015). The recent addition of the capability

of scale awareness to the KF scheme (Alapaty et al., 2012; Bullock et al., 2015; Zheng et al., 2016), resulting in the multiscale KF scheme, appears to enhance its performance in terms of reproducing the diurnal variation of precipitation over the Great Plains. The Tiedtke (CU6) scheme uses a trigger function based on the buoyancy of a undiluted parcel rising from near the surface and a CAPE removal closure based on large-scale convergence (Nordeng, 1995; Zhang et al., 2011); it nicely reproduces the diurnal variation of precipitation (Figure 8), but significantly underestimates total amount of precipitation over the Great Plains (Figure 5g), similar to previously reported (Qiao & Liang, 2015).

Precipitation from the Rockies to the Great Plains shows an eastward propagation (Figures 1a and 9a). The KF (CU1) and BMJ (CU2) schemes that predict afternoon precipitation peaks over both the Rockies and

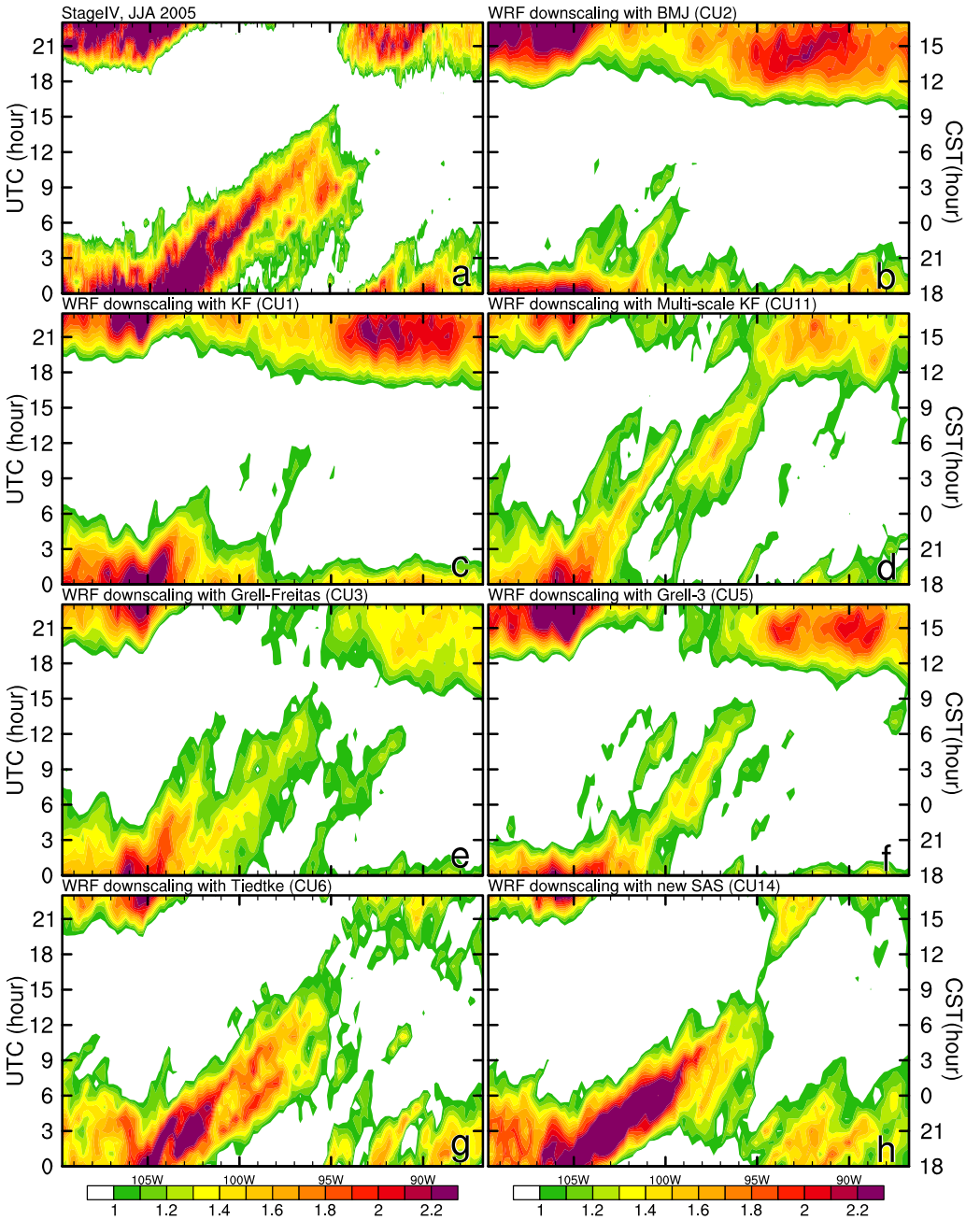

Figure 9. Diurnally average Hovmoller diagrams of normalized hourly precipitation during JJA 2005 from (a) Stage IV observed precipitation and WRF downscaling with different cumulus schemes, i.e., (b) BMJ (CU2), (c) KF (CU1), (d) multiscale KF (CU11), (e) Grell-Freitas (CU3), (f) Grell-3 (CU5), (g) Tiedtke (CU6), and (h) new SAS (CU14).

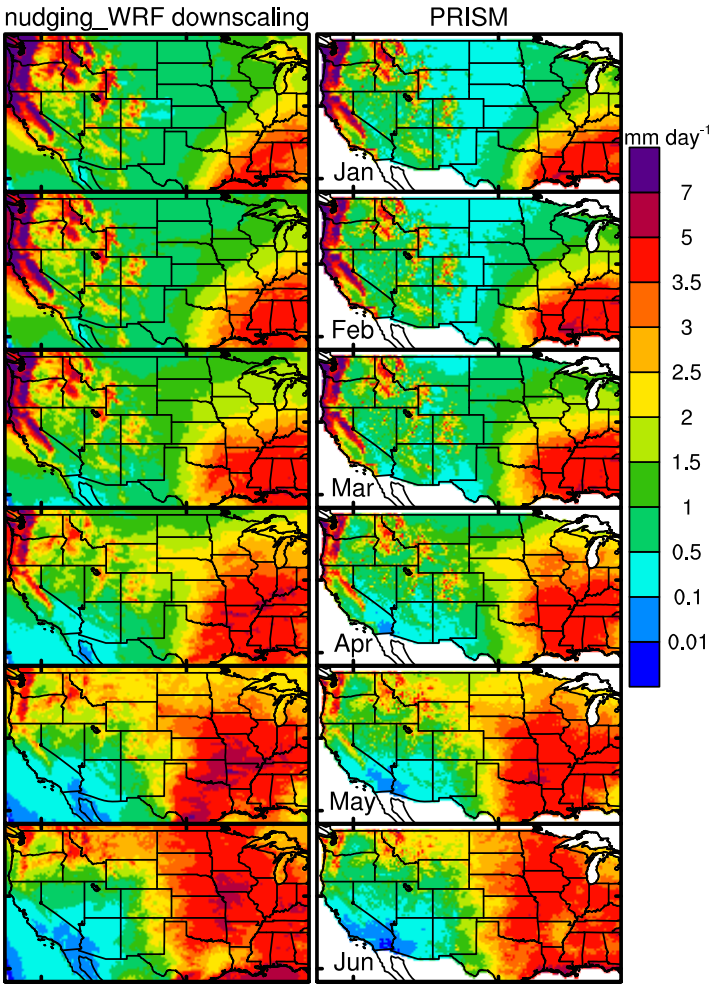

Figure 10. 36 year (1980–2015) monthly climatological precipitation (left) dynamically downscaled with nudging_WRF and (right) retrieved from the PRISM data for the month (top to bottom) January through June.

Great Plains, barely reproduce any eastward propagation of precipitation in the region (Figures 9b and 9c). On the other hand, the schemes that better reproduce the diurnal variation of precipitation across the Rockies and Great Plains (e.g., Grell-Freitas (CU3), Tiedtke (CU6), multiscale KF (CU11), and new SAS (CU14)) also better capture the eastward propagation of precipitation (Figures 9d, 9e, 9g, and 9h). Particularly the scale-aware multiscale KF scheme shows pronounced improvement over its nonscale-aware counterpart (i.e., KF).

3.3. 36 Year (1980–2015) Precipitation Downscaling and Comparison With the NARCCAP WRFG Downscaling

Using what we learned from the prior numerical experiments for summer 2005, we use the control configuration of WRF model as summarized in Table 1 but with the inclusion of spectral nudging (hereafter refer to as nudging_WRF) to downscale precipitation from NCEP/DOE R2 reanalysis for a 36 year period (1980–2015). Figures 10 and 11 compare the downscaled monthly climatological precipitation from January to June and July to December, respectively, during the 36 year period with the PRISM precipitation data. The downscaled results capture the spatial distribution of climatological precipitation amount for each month as well as the monthly variation. Figure 12 shows the annual variation of precipitation amount over the Great Plains. Overall, the WRF downscaling captures the yearly variation of precipitation amount over the Great Plains with a correlation of 0.743 with the PRISM data set, and it overpredicts the precipitation amount with a mean bias (MB) of 0.055 mm d^{-1} and a normalized mean bias (NMB) of 2.4% (see other statistical metrics in Table 5).

We also compare the nudging_WRF downscaling results with those of the 25 year (1980–2004) NARCCAP WRFG to gauge the quality of downscaled precipitation. Note that spectral nudging is not applied in NARCCAP WRFG (Mearns et al., 2012), and detailed configuration of WRFG can be found at http://www.narccap.ucar.edu/data/rcm-characteristics.html. The first 25 year subset of nudging_WRF downscaling is compared with the PRISM data set and NARCCAP WRFG downscaling in Figures 13 and 14. NARCCAP WRFG significantly underpredicts the monthly climatological precipitation over the Great Plains, especially for May through October (Figure 15). In addition, in the months of July and August, NARCCAP WRFG simulates a spatial distribution of precipitation from the Rockies to Great Plains that is not correct (Figure 14). The PRISM data show more precipitation over the Great Plains than over the Rockies while NARCCAP WRFG barely simulates any precipitation over the Great Plains and precipitation that is too high over the Rockies. The warm-season dry biases of NARCCAP WRFG over the Great Plains may be related to the underestimated frequency of nocturnal southerly low-level jets (Tang et al., 2016). As noted earlier, we saw similar poor performance in our previous downscaling experiments without spectral nudging (Sun et al., 2016). With a carefully designed configuration in this current study, however, nudging_WRF provides a better precipitation downscaling over CONUS in nearly every month (Figures 13 and 14), even though it moderately over-produces precipitation over the Great Plains for certain months (particularly May and June, Figure 15). We are also able to substantially alleviate the bias in precipitation locations in warm months (particularly July and August), as compared with those in NARCCAP WRFG and Sun et al. (2016). For example, the mean bias of precipitation of NARCCAP WRFG over the Great Plains (-0.723 mm d^{-1}, -32.1%) is reduced to 0.092 mm d^{-1} (4.1%) in this study (Table 6).

4. Conclusions and Discussion

Accurate precipitation downscaling in the Great Plains remains a great challenge for most RCMs, particularly during the warm months (Liang et al., 2006; Qiao & Liang, 2015; Wang & Kotamarthi, 2014). Most previous

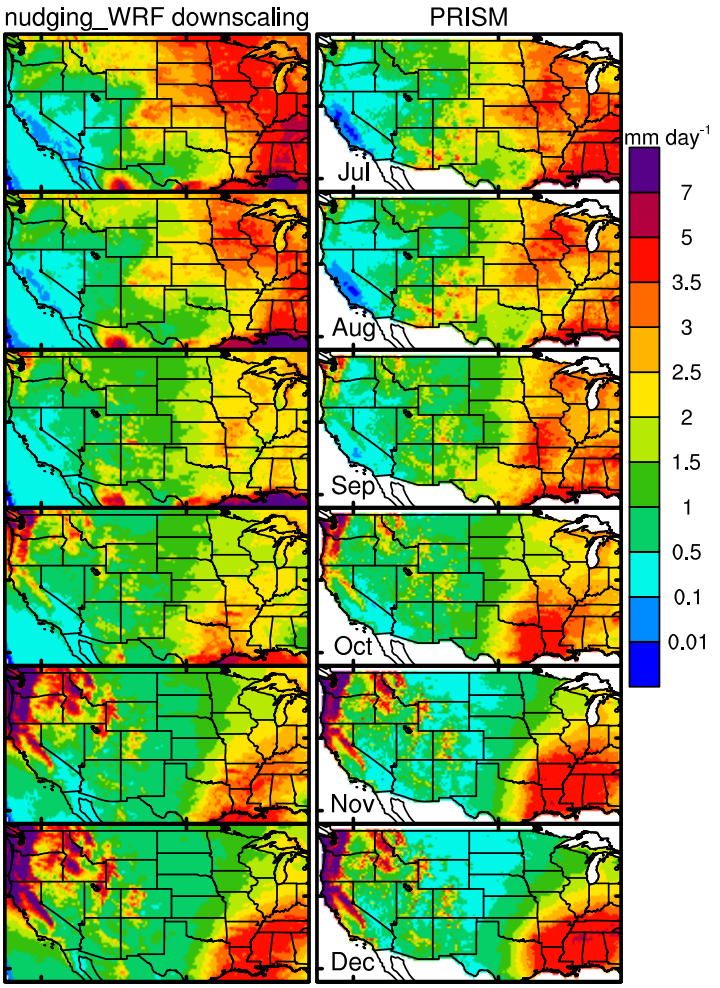

Figure 11. Same as Figure 10, but for the month (top to bottom) July through December.

dynamic downscaling simulations (e.g., Mearns et al., 2012; Sun et al., 2016) significantly underestimate warm-season precipitation in the region. To improve the results, we conduct in this study WRF simulations with different physics parameterization schemes and nudging strategies, first for a representative warm season, in order to identify an optimal configuration or find a plausible solution to the precipitation bias problem. Results show that different cumulus schemes lead to more pronounced difference in simulated precipitation than other tested physics schemes. Simply altering physics schemes (including cumulus schemes, land surface models, PBL schemes, and microphysics schemes) is not enough to alleviate the dry bias over the southern Great Plains, which appears to be related to an anticyclonic circulation anomaly that develops in the long-term simulations over the central and western parts of the continental U.S. The northerly wind anomaly along the eastern flank of this circulation anomaly decreases the prevailing southerly flows over the Great Plains along the western side of the Bermuda High, advecting less moisture from the Gulf of Mexico to the Great Plains. Thus, the anticyclonic circulation anomaly that develops in the continuous, long-term WRF simulation decreases moisture supply to the southern Great Plains and thereby suppresses its associated precipitation.

Interior spectral nudging emerges as an effective solution to reduce the precipitation bias over the Great Plains in the WRF dynamic downscaling. Spectral nudging ensures that the synoptic-scale circulations follow those in the driving fields while simultaneously allowing the RCM (i.e., WRF in this study) to develop small-scale dynamics, which is consistent with the objective of dynamic downscaling, i.e., to produce additional small-scale details under coarse-resolution forcing. Applying spectral nudging effectively suppresses the circulation anomaly in WRF downscaling. As a result, the dry bias over the Great Plains is effectively alleviated and the downscaling performance in reproducing observed precipitation is significantly improved.

With the optimized WRF model configuration, downscaling is carried out from NCEP/DOE R2 forcing using WRF for a 36 year period (1980–

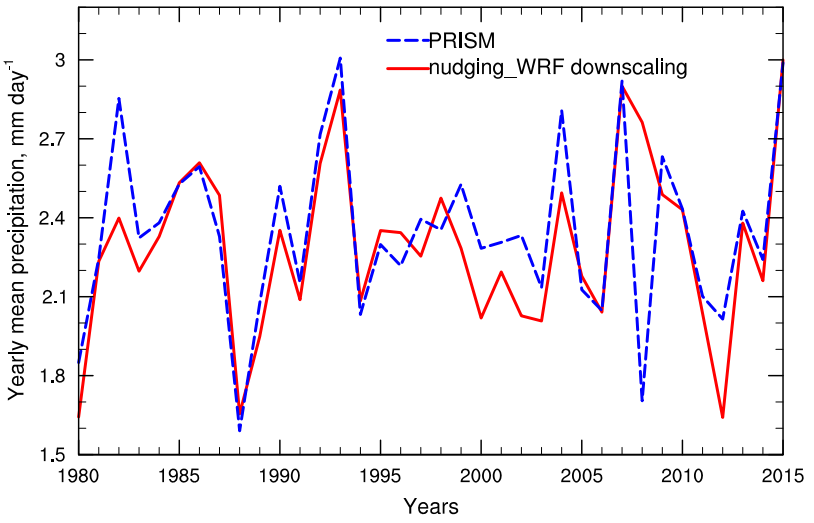

Figure 12. Time series of observed and downscaled yearly mean precipitation rate for the 36 year period (1980–2015) over the Great Plains region, which is marked in the black box in Figure 1.

Table 5
Statistics[a] for the Downscaled Yearly Mean Precipitation Rate Over the Great Plains for the 36 Year Period (1980–2015), Comparing With the PRISM Data

Metrics	Values	Units
Mean observation	2.292	mm d^{-1}
Mean simulation	2.347	mm d^{-1}
Number of data	36	
Correlation coefficient	0.743	
Mean bias (MB)	0.055	mm d^{-1}
Mean absolute gross error (MAGE)	0.150	mm d^{-1}
Root mean-square error (RMSE)	0.240	mm d^{-1}
Normalized mean bias (NMB)	0.024	fraction

[a]Formulae for these statistical metrics can be found in Yu et al. (2006). These statistical metrics are commonly used in numerical model evaluations (Han et al., 2008; Hu et al., 2013; Seigneur et al., 2000).

2015) and compared to corresponding results without spectral nudging. The spatial and temporal distributions of monthly climatological precipitation patterns are captured well in the simulation with spectral nudging. Yearly variation of precipitation amount over the Great Plains is also captured with a correlation of 0.743 with the PRISM precipitation data and, overall, the precipitation amount is only overproduced by 0.055 mm d^{-1} (2.4%). Compared to the downscaling results of NARCCAP WRFG and those reported in Sun et al. (2016), our precipitation downscaling represents a substantial improvement. Even though the testing of the configuration is done for the warm season only, improvements over NARCCAP WRFG are seen throughout the whole year.

The precipitation downscaling can greatly affect downstream impact models. As shown in supporting information, we studied the impact of precipitation downscaling on the trans-state (Oklahoma and Kansas) Oologah Lake watershed of the Great Plains using the VIC model. Because NARCCAP WRFG significantly underestimates precipitation over the Great Plains, especially for Oklahoma and Kansas, the VIC simulations driven by its output consequently significantly underestimate the streamflow at the watershed outlet

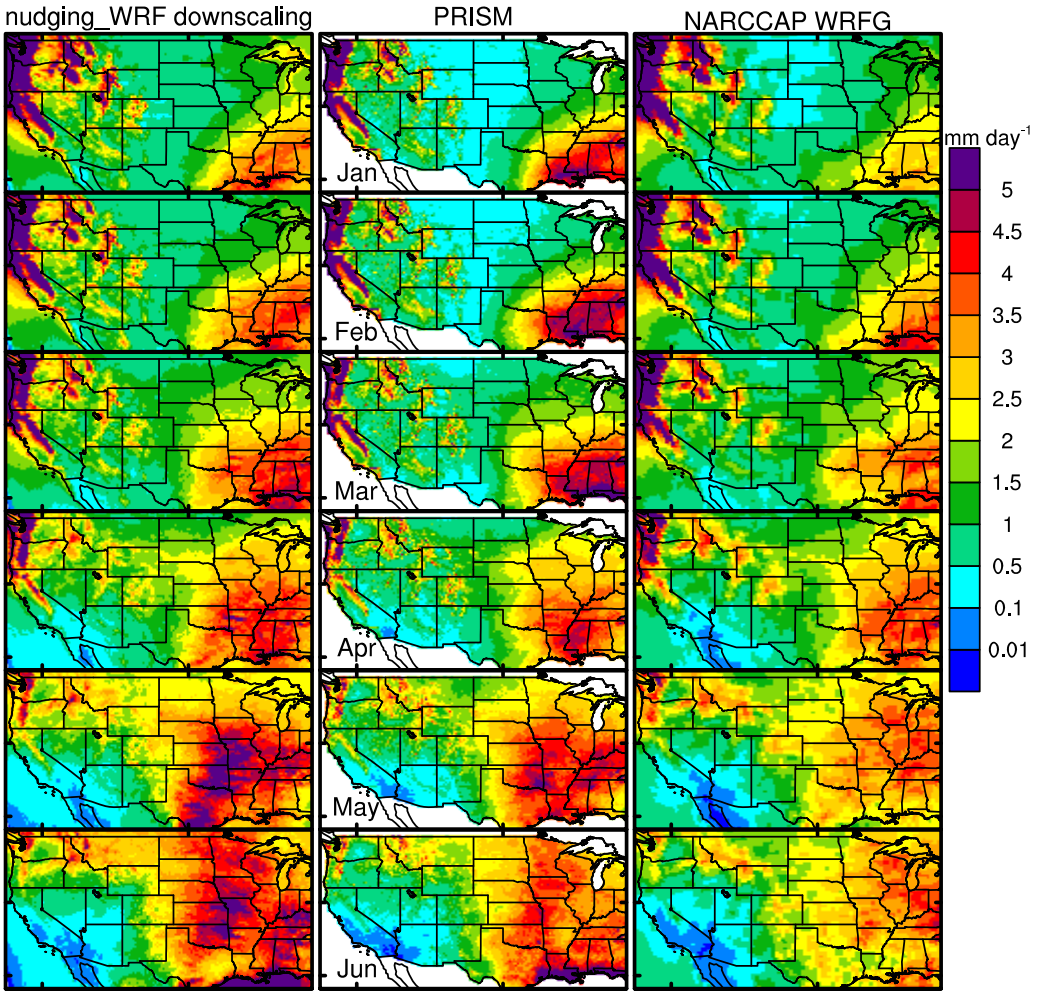

Figure 13. 25 year (1980–2004) monthly climatological precipitation dynamically downscaled (left) with nudging_WRF in this work and (right) with NARCCAP WRFG, and (middle) retrieved from the PRISM data for the month (top to bottom) January through June.

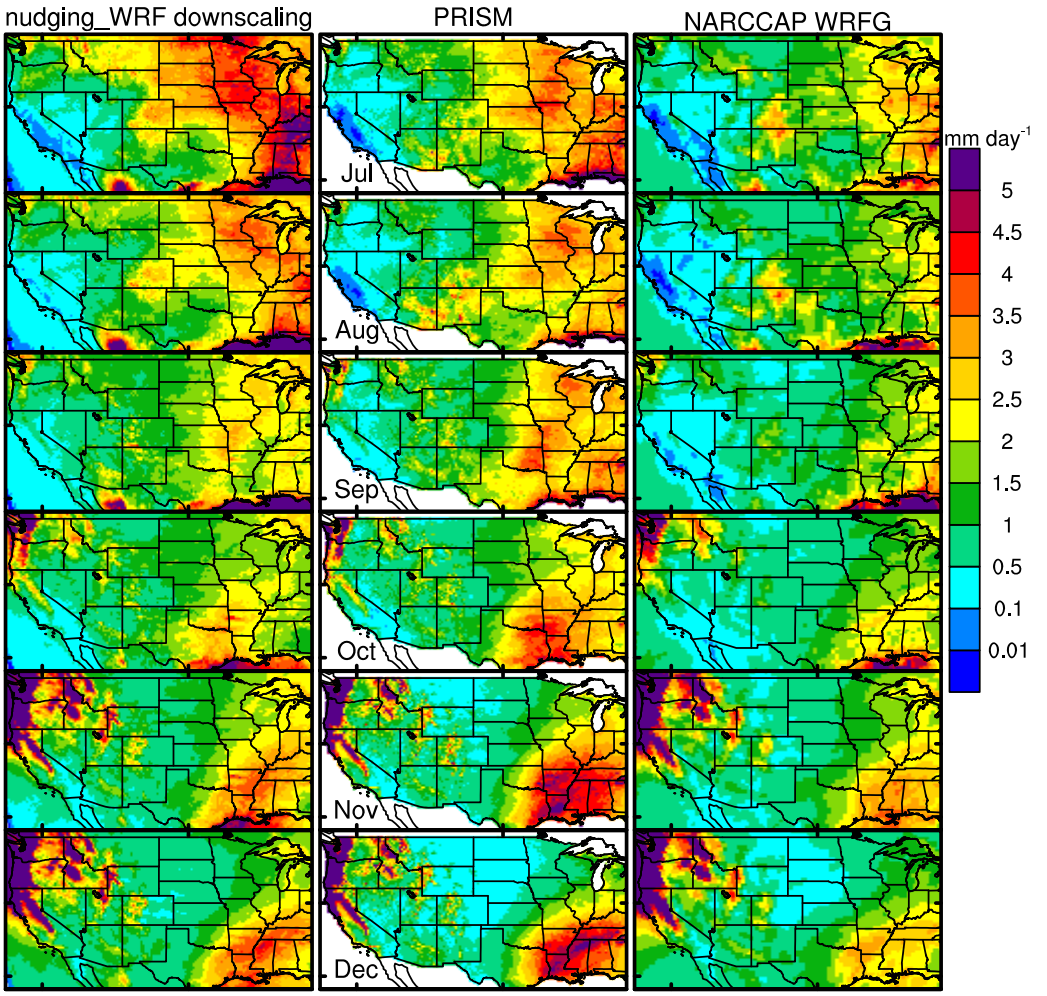

Figure 14. Same as Figure 13, but for the month (top to bottom) July through December.

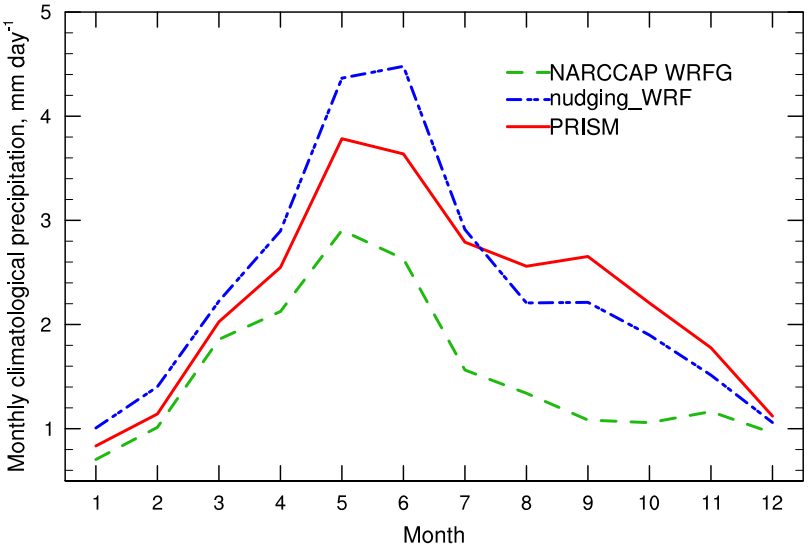

Figure 15. Time series of monthly climatological precipitation rate during the 25 year period (1980–2004) over the Great Plains observed in the PRISM data and downscaled with nudging_WRF in this study and NARCCAP WRFG.

Table 6
Statistics for the Monthly Climatology Precipitation Rate Over the Great Plains for the 25 Year Period (1980–2004) Downscaled by NARCCAP WRFG and nudging_WRF in this Study, Comparing With the PRISM Data

Metrics	NARCCAP WRFG	nudging_WRF downscaling	Units
Mean observation	2.257	2.257	mm d^{-1}
Mean simulation	1.534	2.348	mm d^{-1}
Number of data	12	12	
Correlation coefficient	0.84	0.949	
Mean bias (MB)	−0.723	0.092	mm d^{-1}
Mean absolute gross error (MAGE)	0.723	0.329	mm d^{-1}
Root mean-square error (RMSE)	0.876	0.388	mm d^{-1}
Normalized mean bias (NMB)	−0.321	0.041	fraction

during most of the year, as reported previously by Qiao et al. (2014). With the improved downscaled precipitation from this study, the simulated monthly streamflow rates show a much better agreement with observations.

We note that the WRF downscaling conducted in this study is at a spatial resolution of 20 km, which is larger than the sizes of individual convective storms that frequently occur in the Great Plains. Thus, this method may not be able to accurately simulate convective weather due to its inability to simulate small-scale extreme events (Gao et al., 2012; Gensini & Mote, 2014; Mahoney et al., 2013; Prein et al., 2017; Sun et al., 2016; Zhang et al., 2012). Because of the paramount social and economic impacts these events can cause, higher-resolution dynamical climate downscaling with the ability to capture these small-scale extreme events is warranted to provide the information needed for key local decision-making at relevant (county-level or smaller) scales, particularly for the Great Plains (Harding & Snyder, 2014). Lessons learned from this study may help produce such meaningful higher-resolution dynamic downscaling in the future. When spectral nudging is applied to convection-allowing simulations, as those reported in Sun et al. (2016), further improvements in reproducing features associated with severe weather are expected.

While spectral nudging can alleviate the model bias in an artificial way, the root cause for the model error (i.e., summertime dry bias) over the Great Plains is not revealed clearly with the simulations conducted in this study with different physics schemes. Though not shown here, other sensitivity simulations are also conducted, including changing land properties, different terrain height, different horizontal resolution, and different domain size. The spurious circulation appears initiated west of Mexico (which subsequently leads to a northerly wind anomaly over the Great Plains) and the spurious circulation is related to temperature bias at certain levels, e.g., ∼850, and 500–650 hPa. However, the cause-and-effect relationship between the temperature biases and the spurious circulation yet remains to be revealed in future studies.

Cumulus schemes appear to be the most critical model component to affect precipitation simulations over the Great Plains with a 20 km grid spacing. The scale-aware cumulus schemes (particularly multiscale KF) show better performance than their nonscale-aware counterparts in terms of precipitation amount and timing/propagation. Because of the continuous advancement of computation resources, climate and operational NWP simulations are now advancing from convection-parameterization resolution to convection-permitting resolution, in rare cases to convection-resolving resolution that requires subkilometer grid spacing (Kwon & Hong, 2017). Even though in some convection-permitting simulations (e.g., at 4 km resolution), cumulus schemes are turned off, scale-aware cumulus schemes appear more appropriate in the gray zone (1–15 km), which can bring the convection-parameterization simulations seamlessly converge to convection-resolving simulations as the horizontal grid size is reduced. Also the advantages of scale-aware cumulus schemes over nonscale-aware schemes can be more appreciable in the gray zone. Until cloud-resolving simulations become widely affordable, which may take years, further development/refinement/evaluation of scale-aware cumulus schemes (such as Grell-Freitas and multiscale KF) to improve simulations at the gray-zone resolution (1–15 km) is warranted (Arakawa et al., 2016; Arakawa & Jung, 2011; Gerard et al., 2009; Hong & Dudhia, 2012; Kwon & Hong, 2017; Leung & Gao, 2016).

Acknowledgments
The project described in this manuscript was supported by grant G15AP00131 from the U.S. Geological Survey. Its contents are solely the responsibility of the authors and do not necessarily represent the views of the South Central Climate Science Center or the USGS. This manuscript is submitted for publication with the understanding that the United States Government is authorized to reproduce and distribute reprints for Governmental purposes. The first author was partially supported by grant NA17OAR4590188 from U.S. Department of Commerce, National Oceanic and Atmospheric Administration, and NASA grant NNX17AG11G. The second author was supported by National Science Foundation (NSF) grants AGS-0941491, AGS-1046171, AGS-1046081, and AGS-1261776. Computations were performed at the Texas Advanced Computing Center (TACC) and San Diego Supercomputer Center (SDSC). The reanalysis data set was downloaded from https://rda.ucar.edu/, the PRISM data were downloaded from http://www.prism.oregonstate.edu/historical/, and the Stage IV precipitation data were downloaded from http://data.eol.ucar.edu/codiac/dss/id=21.093. Model data produced from this study have been archived at Center for Analysis and Prediction of Storms, University of Oklahoma, and are available from the authors upon request. Youngsun Jung helped with the spectral analysis. Two anonymous reviewers provided helpful comments that improved the manuscript.

References

Alapaty, K., Herwehe, J. A., Otte, T. L., Nolte, C. G., Bullock, O. R., Mallard, M. S., et al. (2012). Introducing subgrid-scale cloud feedbacks to radiation for regional meteorological and climate modeling. *Geophysical Research Letters*, *39*, L24809. https://doi.org/10.1029/2012GL054031

Alexander, M. A., Scott, J. D., Mahoney, K., & Barsugli, J. (2013). Greenhouse gas-induced changes in summer precipitation over Colorado in NARCCAP regional climate models. *Journal of Climate*, *26*, 8690–8697.

Arakawa, A., & Jung, J. H. (2011). Multiscale modeling of the moist-convective atmosphere—A review. *Atmospheric Research*, *102*, 263–285.

Arakawa, A., Jung, J. H., & Wu, C. M. (2011). Toward unification of the multiscale modeling of the atmosphere. *Atmospheric Chemistry and Physics*, *11*, 3731–3742.

Arakawa, A., Jung, J.-H., & Wu, C.-M. (2016). Multiscale modeling of the moist-convective atmosphere. *Meteorological Monographs*, *56*, 16.1–16.17. https://doi.org/10.1175/amsmonographs-d-15-0014.1

Argueso, D., Hidalgo-Munoz, J. M., Gamiz-Fortis, S. R., Esteban-Parra, M. J., Dudhia, J., & Castro-Diez, Y. (2011). Evaluation of WRF parameterizations for climate studies over Southern Spain using a multistep regionalization. *Journal of Climate*, *24*, 5633–5651.

Arritt, R. W., Rink, T. D., Segal, M., Todey, D. P., Clark, C. A., Mitchell, M. J., et al. (1997). The Great Plains low-level jet during the warm season of 1993. *Monthly Weather Review*, *125*, 2176–2192.

Baldwin, M. E., Kain, J. S., & Kay, M. P. (2002). Properties of the convection scheme in NCEP's eta model that affect forecast sounding interpretation. *Weather and Forecasting*, *17*, 1063–1079.

Berg, A., Findell, K., Lintner, B. R., Gentine, P., & Kerr, C. (2013). Precipitation sensitivity to surface heat fluxes over North America in reanalysis and model data. *Journal of Hydrometeorology*, *14*, 722–743. https://doi.org/10.1175/Jhm-D-12-0111.1

Betts, A. K. (1986). A new convective adjustment scheme. 1. Observational and theoretical basis. *Quarterly Journal of the Royal Meteorological Society*, *112*, 677–691.

Betts, A. K., & Miller, M. J. (1986). A new convective adjustment scheme. 2. Single column tests using gate wave, bomex, atex and arctic airmass data sets. *Quarterly Journal of the Royal Meteorological Society*, *112*, 693–709.

Bougeault, P., & Lacarrere, P. (1989). Parameterization of orography-induced turbulence in a mesobeta-scale model. *Monthly Weather Review*, *117*, 1872–1890. https://doi.org/10.1175/1520-0493(1989)117<1872:Pooiti>2.0.Co;2

Bowden, J. H., Nolte, C. G., & Otte, T. L. (2013). Simulating the impact of the large-scale circulation on the 2-m temperature and precipitation climatology. *Climate Dynamics*, *40*, 1903–1920. https://doi.org/10.1007/s00382-012-1440-y

Bowden, J. H., Otte, T. L., Nolte, C. G., & Otte, M. J. (2012). Examining interior grid nudging techniques using two-way nesting in the WRF model for regional climate modeling. *Journal of Climate*, *25*, 2805–2823. https://doi.org/10.1175/JCLI-D-11-00167.1

Bryan, G. H., Wyngaard, J. C., & Fritsch, J. M. (2003). Resolution requirements for the simulation of deep moist convection. *Monthly Weather Review*, *131*, 2394–2416.

Bukovsky, M. S., Kain, J. S., & Baldwin, M. E. (2006). Bowing convective systems in a popular operational model: Are they for real? *Weather and Forecasting*, *21*, 307–324.

Bukovsky, M. S., & Karoly, D. J. (2009). Precipitation simulations using WRF as a nested regional climate model. *Journal of Applied Meteorology and Climatology*, *48*, 2152–2159. https://doi.org/10.1175/2009jamc2186.1

Bullock, O. R. J., Alapaty, K., Herwehe, J. A., & Kain, J. S. (2015). A dynamically computed convective time scale for the Kain-Fritsch convective parameterization scheme. *Monthly Weather Review*, *143*, 2105–2120. https://doi.org/10.1175/mwr-d-14-00251.1

Bullock, O. R. J., Alapaty, K., Herwehe, J. A., Mallard, M. S., Otte, T. L., Gilliam, R. C., et al. (2014). An observation-based investigation of nudging in WRF for downscaling surface climate information to 12-km grid spacing. *Journal of Applied Meteorology and Climatology*, *53*, 20–33. https://doi.org/10.1175/jamc-d-13-030.1

Caldwell, P. (2010). California wintertime precipitation bias in regional and global climate models. *Journal of Applied Meteorology and Climatology*, *49*, 2147–2158. https://doi.org/10.1175/2010jamc2388.1

Caldwell, P., Chin, H. N. S., Bader, D. C., & Bala, G. (2009). Evaluation of a WRF dynamical downscaling simulation over California. *Climatic Change*, *95*, 499–521.

Carbone, R. E., & Tuttle, J. D. (2008). Rainfall occurrence in the US warm season: The diurnal cycle. *Journal of Climate*, *21*, 4132–4146.

Changnon, S. A. (2001). Thunderstorm rainfall in the conterminous United States. *Bulletin of the American Meteorological Society*, *82*, 1925–1940.

Chen, F., & Dudhia, J. (2001). Coupling an advanced land surface-hydrology model with the Penn State-NCAR MM5 modeling system. Part I: Model implementation and sensitivity. *Monthly Weather Review*, *129*, 569–585. https://doi.org/10.1175/1520-0493(2001)129<0569:Caalsh>2.0.Co;2

Chen, F., Liu, C. H., Dudhia, J., & Chen, M. (2014). A sensitivity study of high-resolution regional climate simulations to three land surface models over the western United States. *Journal of Geophysical Research: Atmospheres*, *119*, 7271–7291. https://doi.org/10.1002/2014JD021827

Choi, I. J., Jin, E. K., Han, J. Y., Kim, S. Y., & Kwon, Y. (2015). Sensitivity of diurnal variation in simulated precipitation during East Asian summer monsoon to cumulus parameterization schemes. *Journal of Geophysical Research: Atmospheres*, *120*, 11971–11987. https://doi.org/10.1002/2015JD023810

Clark, A. J., Gallus, W. A., Xue, M., & Kong, F. Y. (2009). A comparison of precipitation forecast skill between small convection-allowing and large convection-parameterizing ensembles. *Weather and Forecasting*, *24*, 1121–1140. https://doi.org/10.1175/2009waf2222222.1

Dai, A., Giorgi, F., & Trenberth, K. E. (1999). Observed and model-simulated diurnal cycles of precipitation over the contiguous United States. *Journal of Geophysical Research: Atmospheres*, *104*, 6377–6402. https://doi.org/10.1029/98JD02720

Daly, C., Neilson, R. P., & Phillips, D. L. (1994). A statistical topographic model for mapping climatological precipitation over mountainous terrain. *Journal of Applied Meteorology 33*, 140–158. https://doi.org/10.1175/1520-0450(1994)033 < 0140:Astmfm>2.0.Co;2

Davis, C. A., Manning, K. W., Carbone, R. E., Trier, S. B., & Tuttle, J. D. (2003). Coherence of warm-season continental rainfall in numerical weather prediction models. *Monthly Weather Review*, *131*, 2667–2679.

Denis, B., Cote, J., & Laprise, R. (2002). Spectral decomposition of two-dimensional atmospheric fields on limited-area domains using the discrete cosine transform (DCT). *Monthly Weather Review*, *130*, 1812–1829. https://doi.org/10.1175/1520-0493(2002)130<1812:Sdotda>2.0.Co;2

Dickinson, R. E., Errico, R. M., Giorgi, F., & Bates, G. T. (1989). A regional climate model for the Western United-States. *Climatic Change*, *15*, 383–422.

Dudhia, J. (1989). Numerical study of convection observed during the winter monsoon experiment using a mesoscale two-dimensional model. *Journal of the Atmospheric Sciences*, *46*, 3077–3107. https://doi.org/10.1175/1520-0469(1989)046<3077:Nsocod>2.0.Co;2

European Centre for Medium-Range Weather Forecasts (2009). *ERA-Interim project*. Boulder, CO: Research Data Archive at the National Center for Atmospheric Research, Computational and Information Systems Laboratory.

Feng, Z., Leung, L. R., Hagos, S., Houze, R. A., Burleyson, C. D., & Balaguru, K. (2016). More frequent intense and long-lived storms dominate the springtime trend in central US rainfall. *Nature Communications*, *7*, 13429. https://doi.org/10.1038/ncomms13429

Findell, K. L., Gentine, P., Lintner, B. R., & Kerr, C. (2011). Probability of afternoon precipitation in eastern United States and Mexico enhanced by high evaporation. *Nature Geoscience*, *4*, 434–439. https://doi.org/10.1038/Ngeo1174

Flaounas, E., Bastin, S., & Janicot, S. (2011). Regional climate modelling of the 2006 West African monsoon: Sensitivity to convection and planetary boundary layer parameterisation using WRF. *Climate Dynamics*, *36*, 1083–1105.

Fowler, L. D., Skamarock, W. C., Grell, G. A., Freitas, S. R., & Duda, M. G. (2016). Analyzing the Grell-Freitas convection scheme from hydrostatic to nonhydrostatic scales within a global model. *Monthly Weather Review*, *144*, 2285–2306.

Gallus, W. A. (1999). Eta simulations of three extreme precipitation events: Sensitivity to resolution and convective parameterization. *Weather and Forecasting*, *14*, 405–426.

Gao, Y., Fu, J. S., Drake, J. B., Liu, Y., & Lamarque, J. F. (2012). Projected changes of extreme weather events in the eastern United States based on a high resolution climate modeling system. *Environmental Research Letters*, *7*, 044025. https://doi.org/10.1088/1748-9326/7/4/044025

Gao, Y., Leung, L. R., Zhao, C., & Hagos, S. (2017). Sensitivity of US summer precipitation to model resolution and convective parameterizations across gray zone resolutions. *Journal of Geophysical Research: Atmospheres*, *122*, 2714–2733. https://doi.org/10.1002/2016JD025896

Garbrecht, J., Van Liew, M., & Brown, G. O. (2004). Trends in precipitation, streamflow, and evapotranspiration in the Great Plains of the United States. *Journal of Hydrologic Engineering*, *9*, 360–367. https://doi.org/10.1061/(ASCE)1084-0699(2004)9:5(3600)

Garbrecht, J. D., & Rossel, F. E. (2002). Decade-scale precipitation increase in Great Plains at end of 20th century. *Journal of Hydrologic Engineering*, *7*, 64–75. https://doi.org/10.1061/(ASCE)1084-0699(2002)7:1(64)

García-Valdecasas Ojeda, M., Gámiz-Fortis, S., Castro-Díez, R. Y., & Esteban-Parra, M. J. (2017). Evaluation of WRF capability to detect dry and wet periods in Spain using drought indices. *Journal of Geophysical Research: Atmospheres*, *122*, 1569–1594. https://doi.org/10.1002/2016JD025683

Gensini, V. A., & Mote, T. L. (2014). Estimations of hazardous convective weather in the United States using dynamical downscaling. *Journal of Climate*, *27*, 6581–6589. https://doi.org/10.1175/JCLI-D-13-00777.1

Gerard, L., Piriou, J. M., Brozkova, R., & Geleyn, J. F. (2009). Cloud and precipitation parameterization in a meso-gamma-scale operational weather prediction model. *Monthly Weather Review*, *137*, 3960–3977.

Giorgi, F. (1990). Simulation of regional climate using a limited area model nested in a general-circulation model. *Journal of Climate*, *3*, 941–963. https://doi.org/10.1175/1520-0442(1990)003<0941:Sorcua>2.0.Co;2

Gleason, K. L., Lawrimore, J. H., Levinson, D. H., Karl, T. R., & Karoly, D. J. (2008). A revised US climate extremes index. *Journal of Climate*, *21*, 2124–2137. https://doi.org/10.1175/2007JCLI1883.1

Gochis, D. J., Shuttleworth, W. J. A., & Yang, Z. L. (2002). Sensitivity of the modeled North American monsoon regional climate to convective parameterization. *Monthly Weather Review*, *130*, 1282–1298. https://doi.org/10.1175/1520-0493(2002)130<1282:Sotmna>2.0.Co;2

Gochis, D. J., Shuttleworth, W. J. A., & Yang, Z. L. (2003). Hydrometeorological response of the modeled North American monsoon to convective parameterization. *Journal of Hydrometeorology*, *4*, 235–250. https://doi.org/10.1175/1525-7541(2003)4<235:Hrotmn>2.0.Co;2

Gomez, B., & Miguez-Macho, G. (2017). The impact of wave number selection and spin-up time in spectral nudging. *Quarterly Journal of the Royal Meteorological Society*, *143*, 1772–1786. https://doi.org/10.1002/qj.3032

Grell, G. A., & Devenyi, D. (2002). A generalized approach to parameterizing convection combining ensemble and data assimilation techniques. *Geophysical Research Letters*, *29*(14), 1693. https://doi.org/10.1029/2002GL015311

Grell, G. A., & Freitas, S. R. (2014). A scale and aerosol aware stochastic convective parameterization for weather and air quality modeling. *Atmospheric Chemistry and Physics*, *14*, 5233–5250. https://doi.org/10.5194/acp-14-5233-2014

Groisman, P. Y., & Knight, R. W. (2008). Prolonged dry episodes over the conterminous united states: New tendencies emerging during the last 40 years. *Journal of Climate*, *21*, 1850–1862. https://doi.org/10.1175/2007JCLI2013.1

Gutowski, W. J., Arritt, R. W., Kawazoe, S., Flory, D. M., Takle, E. S., Biner, S., et al. (2010). Regional extreme monthly precipitation simulated by NARCCAP RCMs. *Journal of Hydrometeorology*, *11*, 1373–1379. https://doi.org/10.1175/2010jhm1297.1

Halmstad, A., Najafi, M. R., & Moradkhani, H. (2013). Analysis of precipitation extremes with the assessment of regional climate models over the Willamette River Basin, USA. *Hydrological Processes*, *27*, 2579–2590. https://doi.org/10.1002/hyp.9376

Han, J., & Pan, H. L. (2011). Revision of convection and vertical diffusion schemes in the NCEP Global Forecast System. *Weather and Forecasting*, *26*, 520–533. https://doi.org/10.1175/Waf-D-10-05038.1

Han, Z. W., Ueda, H., & An, J. L. (2008). Evaluation and intercomparison of meteorological predictions by five MM5-PBL parameterizations in combination with three land-surface models. *Atmospheric Environment*, *42*, 233–249. https://doi.org/10.1016/j.atmosenv.2007.09.053

Harding, K. J., & Snyder, P. K. (2014). Examining future changes in the character of Central U.S. warm-season precipitation using dynamical downscaling. *Journal of Geophysical Research: Atmospheres*, *119*, 13116–13136. https://doi.org/10.1002/2014JD022575

Harding, K. J., Snyder, P. K., & Liess, S. (2013). Use of dynamical downscaling to improve the simulation of Central US warm season precipitation in CMIP5 models. *Journal of Geophysical Research: Atmospheres*, *118*, 12522–12536. https://doi.org/10.1002/2013JD019994

Harkey, M., & Holloway, T. (2013). Constrained dynamical downscaling for assessment of climate impacts. *Journal of Geophysical Research: Atmospheres*, *118*, 2136–2148. https://doi.org/10.1002/jgrd.50223

Harris, L. M., & Lin, S. J. (2014). Global-to-regional nested grid climate simulations in the GFDL high resolution atmospheric model. *Journal of Climate*, *27*, 4890–4910. https://doi.org/10.1175/JCLI-D-13-00596.1

Helfand, H. M., & Schubert, S. D. (1995). Climatology of the simulated great-plains low-level jet and its contribution to the continental moisture budget of the United-States. *Journal of Climate*, *8*, 784–806.

Herman, G. R., & Schumacher, R. S. (2016). Extreme precipitation in models: An evaluation. *Weather and Forecasting*, *31*, 1853–1879. https://doi.org/10.1175/waf-d-16-0093.1

Herwehe, J. A., Alapaty, K., Spero, T. L., & Nolte, C. G. (2014). Increasing the credibility of regional climate simulations by introducing subgrid-scale cloud-radiation interactions. *Journal of Geophysical Research: Atmospheres*, *119*, 5317–5330.

Higgins, R. W., Yao, Y., Yarosh, E. S., Janowiak, J. E., & Mo, K. C. (1997). Influence of the Great Plains low-level jet on summertime precipitation and moisture transport over the central United States. *Journal of Climate*, *10*, 481–507.

Hong, S.-Y., & Dudhia, J. (2012). Next-generation numerical weather prediction: Bridging parameterization, explicit clouds, and large eddies. *Bulletin of the American Meteorological Society*, *93*, ES6–ES9. https://doi.org/10.1175/2011bams3224.1

Hong, S. Y., Dudhia, J., & Chen, S. H. (2004). A revised approach to ice microphysical processes for the bulk parameterization of clouds and precipitation. *Monthly Weather Review*, *132*, 103–120. https://doi.org/10.1175/1520-0493(2004)132<0103:Aratim>2.0.Co;2

Hong, S. Y., Noh, Y., & Dudhia, J. (2006). A new vertical diffusion package with an explicit treatment of entrainment processes. *Monthly Weather Review*, *134*, 2318–2341. https://doi.org/10.1175/Mwr3199.1

Hu, X.-M., Doughty, D. C., Sanchez, K. J., Joseph, E., & Fuentes, J. D. (2012). Ozone variability in the atmospheric boundary layer in Maryland and its implications for vertical transport model. *Atmospheric Environment*, *46*, 354–364. https://doi.org/10.1016/j.atmosenv.2011.09.054

Hu, X.-M., Klein, P. M., & Xue, M. (2013). Evaluation of the updated YSU planetary boundary layer scheme within WRF for wind resource and air quality assessments. *Journal of Geophysical Research: Atmospheres*, *118*, 10490–10505. https://doi.org/10.1002/jgrd.50823

Hu, X.-M., Nielsen-Gammon, J. W., & Zhang, F. Q. (2010a). Evaluation of three planetary boundary layer schemes in the WRF model. *Journal of Applied Meteorology and Climatology*, *49*, 1831–1844. https://doi.org/10.1175/2010jamc2432.1

Hu, X.-M., Xue, M., & McPherson, R. A. (2017). The importance of soil type contrast in modulating august precipitation distribution near the Edwards Plateau and Balcones Escarpment in Texas. *Journal of Geophysical Research: Atmospheres*, *122*, 10711–10728. https://doi.org/10.1002/2017JD027035

Hu, X.-M., Zhang, F. Q., & Nielsen-Gammon, J. W. (2010b). Ensemble-based simultaneous state and parameter estimation for treatment of mesoscale model error: A real-data study. *Geophysical Research Letters*, *37*, L08802. https://doi.org/10.1029/2010GL043017

Huang, W.-R., Chang, Y.-H., Hsu, H.-H., Cheng, C.-T., & Tu, C.-Y. (2016). Dynamical downscaling simulation and future projection of summer rainfall in Taiwan: Contributions from different types of rain events. *Journal of Geophysical Research: Atmospheres*, *121*, 13973–13988. https://doi.org/10.1002/2016JD025643

Janjic, Z. I. (1994). The step-mountain eta coordinate model—Further developments of the convection, viscous sublayer, and turbulence closure schemes. *Monthly Weather Review*, *122*, 927–945. https://doi.org/10.1175/1520-0493(1994)122<0927:Tsmecm>2.0.Co;2

Jankov, I., Gallus, W. A., Segal, M., Shaw, B., & Koch, S. E. (2005). The impact of different WRF model physical parameterizations and their interactions on warm season MCS rainfall. *Weather and Forecasting*, *20*, 1048–1060. https://doi.org/10.1175/WAF888.1

Kain, J. S. (2004). The Kain-Fritsch convective parameterization: An update. *Journal of Applied Meteorology*, *43*, 170–181. https://doi.org/10.1175/1520-0450(2004)043<0170:Tkcpau>2.0.Co;2

Kanamitsu, M., Ebisuzaki, W., Woollen, J., Yang, S. K., Hnilo, J. J., Fiorino, M., et al. (2002). NCEP-DOE AMIP-II reanalysis (R-2). *Bulletin of the American Meteorological Society*, *83*, 1631–1643. https://doi.org/10.1175/Bams-83-11-1631

Kawazoe, S., & Gutowski, W. J. (2013). Regional, very heavy daily precipitation in NARCCAP simulations. *Journal of Hydrometeorology*, *14*, 1212–1227. https://doi.org/10.1175/Jhm-D-12-068.1

Kendon, E. J., Roberts, N. M., Senior, C. A., & Roberts, M. J. (2012). Realism of rainfall in a very high-resolution regional climate model. *Journal of Climate*, *25*, 5791–5806.

Kessler, E. (1969). On the Distribution and continuity of water substance in atmospheric circulations. In *Meteorological monographs* (Vol. 10, pp. 1–84). Boston, MA: American Meteorological Society.

Kim, J., Waliser, D. E., Mattmann, C. A., Mearns, L. O., Goodale, C. E., Hart, A. F., et al. (2013). Evaluation of the surface climatology over the Conterminous United States in the North American regional climate change assessment program hindcast experiment using a regional climate model evaluation system. *Journal of Climate*, *26*, 5698–5715. https://doi.org/10.1175/JCLI-D-12-00452.1

Klein, C., Heinzeller, D., Bliefernicht, J., & Kunstmann, H. (2015). Variability of West African monsoon patterns generated by a WRF multi-physics ensemble. *Climate Dynamics*, *45*, 2733–2755. https://doi.org/10.1007/s00382-015-2505-5

Klein, P. M., Hu, X.-M., Shapiro, A., & Xue, M. (2016). Linkages between boundary-layer structure and the development of nocturnal low-level jets in Central Oklahoma. *Boundary-Layer Meteorology*, *158*, 383–408. https://doi.org/10.1007/s10546-015-0097-6

Klein, S. A., Jiang, X. N., Boyle, J., Malyshev, S., & Xie, S. C. (2006). Diagnosis of the summertime warm and dry bias over the U.S. Southern Great Plains in the GFDL climate model using a weather forecasting approach. *Geophysical Research Letters*, *33*, L18805. https://doi.org/10.1029/2006GL027567

Kong, F., Xue, M., & Thomas, K. W. (2011). CAPS storm-scale ensemble forecasts in NOAA HWT 2011 Spring Experiment: Sensitivities of WRF model physics. In *12th annual WRF users' workshop* (pp. 6.3). Boston, MA: American Meteorological Society.

Kwon, Y. C., & Hong, S. Y. (2017). A mass-flux cumulus parameterization scheme across gray-zone resolutions. *Monthly Weather Review*, *145*, 583–598.

Lee, H., Waliser, D. E., Ferraro, R., Iguchi, T., Peters-Lidard, C. D., Tian, B., et al. (2017). Evaluating hourly rainfall characteristics over the U.S. Great Plains in dynamically downscaled climate model simulations using NASA-Unified WRF. *Journal of Geophysical Research: Atmospheres*, *122*, 7371–7384. https://doi.org/10.1002/2017JD026564

Lee, M. I., Schubert, S. D., Suarez, M. J., Held, I. M., Lau, N., Ploshay, J. J., et al. (2007a). An analysis of the warm-season diurnal cycle over the continental united states and northern Mexico in general circulation models. *Journal of Hydrometeorology*, *8*, 344–366.

Lee, M. I., Schubert, S. D., Suarez, M. J., Held, I. M., Kumar, A., Bell, T. L., et al. (2007b). Sensitivity to horizontal resolution in the AGCM simulations of warm season diurnal cycle of precipitation over the United States and northern Mexico. *Journal of Climate*, *20*, 1862–1881. https://doi.org/10.1175/JCLI4090.1

Lee, M. I., Schubert, S. D., Suarez, M. J., Schemm, J. K. E., Pan, H. L., Han, J., et al. (2008). Role of convection triggers in the simulation of the diurnal cycle of precipitation over the United States Great Plains in a general circulation model. *Journal of Geophysical Research: Atmospheres*, *113*, D02111. https://doi.org/10.1029/2007JD008984

Leung, L. R., & Gao, Y. (2016). Regional downscaling of S2S prediction: Past lessons and future prospects. *CLIVAR Variations*, *14*(4), 13–17.

Leung, L. R., Kuo, Y. H., & Tribbia, J. (2006). Research needs and directions of regional climate modeling using WRF and CCSM. *Bulletin of the American Meteorological Society*, *87*, 1747–1751. https://doi.org/10.1175/Bams-887-12-1747

Liang, X., Lettenmaier, D. P., Wood, E. F., & Burges, S. J. (1994). A simple hydrologically based model of land-surface water and energy fluxes for general-circulation models. *Journal of Geophysical Research: Atmospheres*, *99*, 14415–14428. https://doi.org/10.1029/94JD00483

Liang, X., Wood, E. F., & Lettenmaier, D. P. (1999). Modeling ground heat flux in land surface parameterization schemes. *Journal of Geophysical Research: Atmospheres*, *104*, 9581–9600. https://doi.org/10.1029/98JD02307

Liang, X. Z., Li, L., Dai, A., & Kunkel, K. E. (2004b). Regional climate model simulation of summer precipitation diurnal cycle over the United States. *Geophysical Research Letters*, *31*, L24208. https://doi.org/10.1029/2004GL021054

Liang, X.-Z., Li, L., Kunkel, K. E., Ting, M., & Wang, J. X. L. (2004a). Regional climate model simulation of U.S. precipitation during 1982–2002. Part I: Annual cycle. *Journal of Climate*, *17*, 3510–3529. https://doi.org/10.1175/1520-0442(2004)017<3510:RCMSOU>2.0.CO;2

Liang, X. Z., Pan, J. P., Zhu, J. H., Kunkel, K. E., Wang, J. X. L., & Dai, A. (2006). Regional climate model downscaling of the U.S. summer climate and future change. *Journal of Geophysical Research: Atmospheres*, *111*, D10108. https://doi.org/10.1029/2005JD006685

Lim, K. S. S., Hong, S. Y., Yoon, J. H., & Han, J. (2014). Simulation of the summer monsoon rainfall over East Asia using the NCEP GFS cumulus parameterization at different horizontal resolutions. *Weather and Forecasting*, *29*, 1143–1154.

Lin, Y. (2011). *GCIP/EOP surface: Precipitation NCEP/EMC 4 km Gridded Data (GRIB) Stage IV data*. UNEO Laboratory, Ed., UCAR/NCAR—Earth Observing Laboratory. https://doi.org/10.5065/D6PG1QDD

Liu, P., Tsimpidi, A. P., Hu, Y., Stone, B., Russell, A. G., & Nenes, A. (2012). Differences between downscaling with spectral and grid nudging using WRF. *Atmospheric Chemistry and Physics*, *12*, 3601–3610. https://doi.org/10.5194/acp-12-3601-2012

Lo, J. C. F., Yang, Z. L., & Pielke, R. A. (2008). Assessment of three dynamical climate downscaling methods using the Weather Research and Forecasting (WRF) model. *Journal of Geophysical Research: Atmospheres*, *113*, D09112. https://doi.org/10.1029/2007JD009216

Lynn, B. H., Healy, R., & Druyan, L. M. (2009). Quantifying the sensitivity of simulated climate change to model configuration. *Climatic Change*, *92*, 275–298.

Ma, H. Y., Xie, S., Klein, S. A., Williams, K. D., Boyle, J. S., Bony, S., et al. (2014). On the correspondence between mean forecast errors and climate errors in CMIP5 models. *Journal of Climate*, *27*, 1781–1798. https://doi.org/10.1175/JCLI-D-13-00474.1

Mabuchi, K., Sato, Y., & Kida, H. (2002). Verification of the climatic features of a regional climate model with BAIM. *Journal of the Meteorological Society of Japan*, *80*, 621–644. https://doi.org/10.2151/jmsj.80.621

Mahoney, K., Alexander, M., Scott, J. D., & Barsugli, J. (2013). High-resolution downscaled simulations of warm-season extreme precipitation events in the Colorado Front range under past and future climates. *Journal of Climate*, *26*, 8671–8689.

Mailhot, A., Beauregard, I., Talbot, G., Caya, D., & Biner, S. (2012). Future changes in intense precipitation over Canada assessed from multi-model NARCCAP ensemble simulations. *International Journal of Climatology*, *32*, 1151–1163. https://doi.org/10.1002/joc.2343

Martynov, A., Laprise, R., Sushama, L., Winger, K., Separovic, L., & Dugas, B. (2013). Reanalysis-driven climate simulation over CORDEX North America domain using the Canadian Regional Climate Model, version 5: Model performance evaluation. *Climate Dynamics*, *41*, 2973–3005. https://doi.org/10.1007/s00382-013-1778-9

Mearns, L. O., Arritt, R., Biner, S., Bukovsky, M. S., McGinnis, S., Sain, S., et al. (2012). The North American regional climate change assessment program overview of phase I results. *Bulletin of the American Meteorological Society*, *93*, 1337–1362.

Mesinger, F., DiMego, G., Kalnay, E., Mitchell, K., Shafran, P. C., Ebisuzaki, W., et al. (2006). North American regional reanalysis. *Bulletin of the American Meteorological Society*, *87*, 343–360. https://doi.org/10.1175/Bams-87-3-343

Michelson, S. A., & Bao, J. W. (2008). Sensitivity of low-level winds simulated by the WRF model in California's Central Valley to uncertainties in the large-scale forcing and soil initialization. *Journal of Applied Meteorology and Climatology*, *47*, 3131–3149. https://doi.org/10.1175/2008jamc1782.1

Miguez-Macho, G., Stenchikov, G. L., & Robock, A. (2004). Spectral nudging to eliminate the effects of domain position and geometry in regional climate model simulations. *Journal of Geophysical Research: Atmospheres*, *109*, D13104. https://doi.org/10.1029/2003JD004495

Miguez-Macho, G., Stenchikov, G. L., & Robock, A. (2005). Regional climate simulations over North America: Interaction of local processes with improved large-scale flow. *Journal of Climate*, *18*, 1227–1246. https://doi.org/10.1175/JCLI3369.1

Mlawer, E. J., Taubman, S. J., Brown, P. D., Iacono, M. J., & Clough, S. A. (1997). Radiative transfer for inhomogeneous atmospheres: RRTM, a validated correlated-k model for the longwave. *Journal of Geophysical Research: Atmospheres*, *102*, 16663–16682. https://doi.org/10.1029/97JD00237

Morrison, H., Thompson, G., & Tatarskii, V. (2009). Impact of cloud microphysics on the development of trailing stratiform precipitation in a simulated squall line: Comparison of one- and two-moment schemes. *Monthly Weather Review*, *137*, 991–1007. https://doi.org/10.1175/2008mwr2556.1

Nelson, B. R., Prat, O. P., Seo, D. J., & Habib, E. (2016). Assessment and implications of NCEP Stage IV quantitative precipitation estimates for product intercomparisons. *Weather and Forecasting*, *31*, 371–394. https://doi.org/10.1175/Waf-D-14-00112.1

Nielsen-Gammon, J. W., Hu, X. M., Zhang, F. Q., & Pleim, J. E. (2010). Evaluation of planetary boundary layer scheme sensitivities for the purpose of parameter estimation. *Monthly Weather Review*, *138*, 3400–3417. https://doi.org/10.1175/2010mwr3292.1

Nordeng, T. E. (1995). *Extended versions of the convective parameterization scheme at ECMWF and their impact on the mean and transient activity of the model in the Tropics* (Tech. Memo. 206, 41 pp.). ECMWF Research Department.

Omrani, H., Drobinski, P., & Dubos, T. (2013). Optimal nudging strategies in regional climate modelling: Investigation in a Big-Brother experiment over the European and Mediterranean regions. *Climate Dynamics*, *41*, 2451–2470. https://doi.org/10.1007/s00382-012-1615-6

Otte, T. L., Nolte, C. G., Otte, M. J., & Bowden, J. H. (2012). Does nudging squelch the extremes in regional climate modeling? *Journal of Climate*, *25*, 7046–7066. https://doi.org/10.1175/JCLI-D-12-00048.1

Pan, H.-L., & Wu, W.-S. (1995). *Implementing a mass flux convective parameterization package for the NMC medium-range forecast model* (Office Note 409, 40 pp.). Boulder, CO: U.S. Department of Commerce National Oceanic and Atmospheric Administration.

Pan, Z. T., Takle, E., Gutowski, W., & Turner, R. (1999). Long simulation of regional climate as a sequence of short segments. *Monthly Weather Review*, *127*, 308–321. https://doi.org/10.1175/1520-0493(1999)127 < 0308:Lsorca>2.0.Co;2

Paul, S., Ghosh, S., Oglesby, R., Pathak, A., Chandrasekharan, A., & Ramsankaran, R. A. A. J. (2016). Weakening of Indian summer monsoon rainfall due to changes in land use land cover. *Scientific Reports*, *6*, 32177. https://doi.org/10.1038/srep32177

Pei, L. S., Moore, N., Zhong, S. Y., Luo, L. F., Hyndman, D. W., Heilman, W. E., et al. (2014). WRF model sensitivity to land surface model and cumulus parameterization under short-term climate extremes over the Southern Great Plains of the United States. *Journal of Climate*, *27*, 7703–7724.

Pieri, A. B., von Hardenberg, J., Parodi, A., & Provenzale, A. (2015). Sensitivity of precipitation statistics to resolution, microphysics, and convective parameterization: A case study with the high-resolution WRF climate model over Europe. *Journal of Hydrometeorology*, *16*, 1857–1872.

Pleim, J. E. (2007). A combined local and nonlocal closure model for the atmospheric boundary layer. Part I: Model description and testing. *Journal of Applied Meteorology and Climatology*, *46*, 1383–1395. https://doi.org/10.1175/Jam2539.1

Pohl, B., Rouault, M., & Sen Roy, S. (2014). Simulation of the annual and diurnal cycles of rainfall over South Africa by a regional climate model. *Climate Dynamics*, *43*, 2207–2226. https://doi.org/10.1007/s00382-013-2046-8

Prat, O. P., & Nelson, B. R. (2015). Evaluation of precipitation estimates over CONUS derived from satellite, radar, and rain gauge data sets at daily to annual scales (2002–2012). *Hydrology and Earth System Sciences*, *19*, 2037–2056. https://doi.org/10.5194/hess-19-2037-2015

Prein, A. F., Langhans, W., Fosser, G., Ferrone, A., Ban, N., Goergen, K., et al. (2015). A review on regional convection-permitting climate modeling: Demonstrations, prospects, and challenges. *Reviews of Geophysics*, *53*, 323–361.

Prein, A. F., Rasmussen, R. M., Ikeda, K., Liu, C., Clark, M. P., & Holland, G. J. (2017). The future intensification of hourly precipitation extremes. *Nature Climate Change*, *7*, 48–52. https://doi.org/10.1038/nclimate3168

Qian, J. H., Seth, A., & Zebiak, S. (2003). Reinitialized versus continuous simulations for regional climate downscaling. *Monthly Weather Review*, *131*, 2857–2874. https://doi.org/10.1175/1520-0493(2003)131 < 2857:Rvcsfr>2.0.Co;2

Qiao, F. X., & Liang, X. Z. (2015). Effects of cumulus parameterizations on predictions of summer flood in the Central United States. *Climate Dynamics*, *45*, 727–744. https://doi.org/10.1007/s00382-014-2301-7

Qiao, F. X., & Liang, X. Z. (2016). Effects of cumulus parameterization closures on simulations of summer precipitation over the United States coastal oceans. *Journal of Advances in Modeling Earth Systems*, *8*, 764–785. https://doi.org/10.1002/2015MS000621

Qiao, L., Hong, Y., McPherson, R., Shafer, M., Gade, D., Williams, D., et al. (2014). Climate change and hydrological response in the trans-State Oologah Lake watershed-evaluating dynamically downscaled NARCCAP and statistically downscaled CMIP3 simulations with VIC model. *Water Resource Management*, *28*, 3291–3305. https://doi.org/10.1007/s11269-014-0678-z

Ramsey, N. R., Klein, P. M., & Moore, B. (2014). The impact of meteorological parameters on urban air quality. *Atmospheric Environment*, *86*, 58–67. https://doi.org/10.1016/j.atmosenv.2013.12.006

Schumacher, R. S., Clark, A. J., Xue, M., & Kong, F. Y. (2013). Factors influencing the development and maintenance of nocturnal heavy-rain-producing convective systems in a storm-scale ensemble. *Monthly Weather Review*, *141*, 2778–2801. https://doi.org/10.1175/Mwr-D-12-00239.1

Seigneur, C., Pun, B., Pai, P., Louis, J.-F., Solomon, P., Emery, C., et al. (2000). Guidance for the performance evaluation of three-dimensional air quality modeling systems for particulate matter and visibility. *Journal of the Air & Waste Management Association*, *50*, 588–599.

Shafer, M., Ojima, D., Antle, J. M., Kluck, D., McPherson, R., Petersen, S., et al. (2014). Ch. 19: Great Plains. In J. M. Melillo, T. Richmond, & G. W. Yohe (Eds.), *Climate change impacts in the United States: The third national climate assessment* (pp. 441–461), U.S. Global Change Research Program. Retrieved from https://nca2014.globalchange.gov/downloads

Shin, H. H., & Hong, S. Y. (2015). Representation of the subgrid-scale turbulent transport in convective boundary layers at gray-zone resolutions. *Monthly Weather Review*, *143*, 250–271. https://doi.org/10.1175/Mwr-D-14-00116.1

Sikder, S., & Hossain, F. (2016). Assessment of the Weather Research and Forecasting model generalized parameterization schemes for advancement of precipitation forecasting in monsoon-driven river basins. *Journal of Advances in Modeling Earth Systems*, *8*, 1210–1228.

Singh, D., Tsiang, M., Rajaratnam, B., & Diffenbaugh, N. S. (2013). Precipitation extremes over the continental United States in a transient, high-resolution, ensemble climate model experiment. *Journal of Geophysical Research: Atmospheres*, *118*, 7063–7086. https://doi.org/10.1002/jgrd.50543

Skamarock, W. C., & Klemp, J. B. (2008). A time-split nonhydrostatic atmospheric model for Weather Research and Forecasting applications. *Journal of Computational Physics*, *227*, 3465–3485. https://doi.org/10.1016/j.jcp.2007.01.037

Skamarock, W. C., Klemp, J. B., Dudhia, J., Gill, D. O., Barker, D. M., Duda, M. G., et al. (2008). *A description of the advanced research WRF version 3* (NCAR Tech. Note TN-475_STR. 113). Boulder, CO: National Center for Atmospheric Research.

Smirnova, T. G., Brown, J. M., Benjamin, S. G., & Kim, D. (2000). Parameterization of cold-season processes in the MAPS land-surface scheme. *Journal of Geophysical Research: Atmospheres*, *105*, 4077–4086. https://doi.org/10.1029/1999JD901047

Soares, P. M. M., Cardoso, R. M., Miranda, P. M. A., de Medeiros, J., Belo-Pereira, M., & Espirito-Santo, F. (2012). WRF high resolution dynamical downscaling of ERA-Interim for Portugal. *Climate Dynamics*, *39*, 2497–2522. https://doi.org/10.1007/s00382-012-1315-2

Spero, T. L., Otte, M. J., Bowden, J. H., & Nolte, C. G. (2014). Improving the representation of clouds, radiation, and precipitation using spectral nudging in the Weather Research and Forecasting model. *Journal of Geophysical Research: Atmospheres*, *119*, 11682–11694. https://doi.org/10.1002/2014JD022173

Steiner, J. L., Starks, P. J., Garbrecht, J. D., Moriasi, D. N., Zhang, X., Schneider, J. M., et al. (2014). Long-term environmental research: The Upper Washita River Experimental Watersheds, Oklahoma, USA. *Journal of Environmental Quality*, *43*, 1227–1238. https://doi.org/10.2134/jeq2014.05.0229

Sun, X., Xue, M., Brotzge, J., McPherson, R. A., Hu, X.-M., & Yang, X.-Q. (2016). An evaluation of dynamical downscaling of Central Plains summer precipitation using a WRF-based regional climate model at a convection-permitting 4 km resolution. *Journal of Geophysical Research: Atmospheres*, *121*, 13801–13825. https://doi.org/10.1002/2016JD024796

Surcel, M., Zawadzki, I., & Yau, M. K. (2014). On the filtering properties of ensemble averaging for storm-scale precipitation forecasts. *Monthly Weather Review*, *142*, 1093–1105. https://doi.org/10.1175/Mwr-D-13-00134.1

Tang, Y., Zhong, S. Y., Winker, J. A., & Walters, C. K. (2016). Evaluation of the southerly low-level jet climatology for the central United States as simulated by NARCCAP regional climate models. *International Journal of Climatology*, *36*, 4338–4357. https://doi.org/10.1002/joc.4636

Tian, B., Lee, H., Waliser, D. E., Ferraro, R., Kim, J., Case, J., et al. (2017). Development of a model performance metric and its application to assess summer precipitation over the U.S. Great Plains in downscaled climate simulations. *Journal of Hydrometeorology*, *18*, 2781–2799. https://doi.org/10.1175/jhm-d-17-0045.1

Tiedtke, M., (1989). A comprehensive mass flux scheme for cumulus parameterization in large-scale models. *Monthly Weather Review*, *1*, 1779–1800. https://doi.org/10.1175/1520-0493(1989)117 < 1779:Acmfsf>2.0.Co;2

Trier, S. B., Chen, F., Manning, K. W., LeMone, M. A., & Davis, C. A. (2008). Sensitivity of the PBL and precipitation in 12-day simulations of warm-season convection using different land surface models and soil wetness conditions. *Monthly Weather Review*, *136*, 2321–2343. https://doi.org/10.1175/2007mwr2289.1

Trier, S. B., LeMone, M. A., Chen, F., & Manning, K. W. (2011). Effects of surface heat and moisture exchange on ARW-WRF warm-season precipitation forecasts over the Central United States. *Weather and Forecasting*, *26*, 3–25. https://doi.org/10.1175/2010waf2222426.1

Tripathi, O. P., & Dominguez, F. (2013). Effects of spatial resolution in the simulation of daily and subdaily precipitation in the southwestern US. *Journal of Geophysical Research: Atmospheres*, *118*, 7591–7605. https://doi.org/10.1002/jgrd.50590

Vidale, P. L., Luthi, Frei, D. C., Seneviratne, S. I., & Schar, C. (2003). Predictability and uncertainty in a regional climate model. *Journal of Geophysical Research*, *108*(D18), 4586. https://doi.org/10.1029/2002JD002810

Vincent, C. L., & Hahmann, A. N. (2015). The impact of grid and spectral nudging on the variance of the near-surface wind speed. *Journal of Applied Meteorology and Climatology*, *54*, 1021–1038. https://doi.org/10.1175/Jamc-D-14-0047.1

von Storch, H., Langenberg, H., & Feser, F. (2000). A spectral nudging technique for dynamical downscaling purposes. *Monthly Weather Review*, *128*, 3664–3673. https://doi.org/10.1175/1520-0493(2000)128 < 3664:Asntfd>2.0.Co;2

Wang, J. L., & Kotamarthi, V. R. (2013). Assessment of dynamical downscaling in near-surface fields with different spectral nudging approaches using the Nested Regional Climate Model (NRCM). *Journal of Applied Meteorology and Climatology*, *52*, 1576–1591. https://doi.org/10.1175/Jamc-D-12-0302.1

Wang, J. L., & Kotamarthi, V. R. (2014). Downscaling with a nested regional climate model in near-surface fields over the contiguous United States. *Journal of Geophysical Research: Atmospheres*, *119*, 8778–8797. https://doi.org/10.1002/2014JD021696

Wang, S. Y., Gillies, R. R., Takle, E. S., & Gutowski, W. J. (2009). Evaluation of precipitation in the Intermountain Region as simulated by the NARCCAP regional climate models. *Geophysical Research Letters*, *36*, L11704. https://doi.org/10.1029/2009GL037930

Wang, Y. C., Pan, H. L., & Hsu, H. H. (2015). Impacts of the triggering function of cumulus parameterization on warm-season diurnal rainfall cycles at the Atmospheric Radiation Measurement Southern Great Plains site. *Journal of Geophysical Research: Atmospheres*, *120*, 10681–10702. https://doi.org/10.1002/2015JD023337

Wehner, M. F. (2013). Very extreme seasonal precipitation in the NARCCAP ensemble: Model performance and projections. *Climate Dynamics*, *40*, 59–80. https://doi.org/10.1007/s00382-012-1393-1

Wi, S., Dominguez, F., Durcik, M., Valdes, J., Diaz, H. F., & Castro, C. L. (2012). Climate change projection of snowfall in the Colorado River Basin using dynamical downscaling. *Water Resources Research*, *48*, W05504. https://doi.org/10.1029/2011WR010674

Wyngaard, J. C. (2004). Toward numerical modeling in the "terra incognita". *Journal of the Atmospheric Sciences*, *61*, 1816–1826.

Xie, S. C., & Zhang, M. H. (2000). Impact of the convection triggering function on single-column model simulations. *Journal of Geophysical Research*, *105*, 14983–14996. https://doi.org/10.1029/2000JD900170

Xue, M., Kong, F., Thomas, K., Gao, J., Wang, Y., Brewster, K., et al. (2009). CAPS realtime multi-model convection-allowing ensemble and 1-km convection-resolving forecasts for the NOAA Hazardous Weather Testbed 2009 Spring experiment. In *23rd conference on weather analysis and forecasting/19th conference on numerical weather prediction* (Paper 16). Boston, MA: American Meteorological Society.

Xue, M., Kong, F., Thomas, K. W., Wang, Y., Brewster, K., Gao, J., et al. (2010). CAPS realtime storm scale ensemble and high resolution forecasts for the NOAA Hazardous Weather Testbed 2010 Spring experiment. In *24th conference on weather analysis and forecasting/20th conference on numerical weather prediction* (Paper 7B.3). Boston, MA: American Meteorological Society.

Xue, M., Kong, F., Weber, D., Thomas, K. W., Wang, Y., Brewster, K., et al. (2007). CAPS realtime storm-scale ensemble and high-resolution forecasts as part of the NOAA Hazardous Weather Testbed 2007 Spring experiment. In *22nd conference on weather analysis and forecasting/18th conference on numerical weather prediction*. Boston, MA: American Meteorological Society.

Xue, Y. K., Janjic, Z., Dudhia, J., Vasic, R., & De Sales, F. (2014). A review on regional dynamical downscaling in intraseasonal to seasonal simulation/prediction and major factors that affect downscaling ability. *Atmospheric Research*, *147*, 68–85.

Yamada, T. J., Lee, M. I., Kanamitsu, M., & Kanamaru, H. (2012). Diurnal characteristics of rainfall over the contiguous United States and Northern Mexico in the dynamically downscaled reanalysis dataset (US10). *Journal of Hydrometeorology*, *13*, 1142–1148. https://doi.org/10.1175/Jhm-D-11-0121.1

Yu, S. C., Eder, B., Dennis, R., Chu, S. H., & Schwartz, S. E. (2006). New unbiased symmetric metrics for evaluation of air quality models. *Atmospheric Science Letters*, *7*, 26–34. https://doi.org/10.1002/asl.125

Zhang, C. X., Wang, Y. Q., & Hamilton, K. (2011). Improved representation of boundary layer clouds over the Southeast Pacific in ARW-WRF using a modified Tiedtke cumulus parameterization scheme. *Monthly Weather Review*, *139*, 3489–3513.

Zhang, C. X., Wang, Y. Q., Lauer, A., & Hamilton, K. (2012). Configuration and evaluation of the WRF model for the study of Hawaiian regional climate. *Monthly Weather Review*, *140*, 3259–3277.

Zhang, G. J. (2002). Convective quasi-equilibrium in midlatitude continental environment and its effect on convective parameterization. *Journal of Geophysical Research: Atmospheres*, *107*(D14), 4220. https://doi.org/10.1029/2001JD001005

Zhang, G. J. (2003). Roles of tropospheric and boundary layer forcing in the diurnal cycle of convection in the U.S. southern great plains. *Geophysical Research Letters*, *30*(24), 2281. https://doi.org/10.1029/2003GL018554

Zhang, X. D., He, J. X., Zhang, J., Polyakov, I., Gerdes, R., Inoue, J., et al. (2013). Enhanced poleward moisture transport and amplified northern high-latitude wetting trend. *Nature Climate Change*, *3*, 47–51. https://doi.org/10.1038/Nclimate1631

Zhang, Y. X., Duliere, V., Mote, P. W., & Salathe, E. P. (2009). Evaluation of WRF and HadRM mesoscale climate simulations over the US Pacific Northwest. *Journal of Climate*, *22*, 5511–5526. https://doi.org/10.1175/2009JCLI2875.1

Zheng, Y., Alapaty, K., Herwehe, J. A., Del Genio, A. D., & Niyogi, D. (2016). Improving high-resolution weather forecasts using the Weather Research and Forecasting (WRF) model with an updated Kain-Fritsch scheme. *Monthly Weather Review*, *144*, 833–860. https://doi.org/10.1175/Mwr-D-15-0005.1

Zhou, B., Xue, M., & Zhu, K. (2017). A grid-refinement-based approach for modeling the convective boundary layer in the gray zone: A pilot study. *Journal of the Atmospheric Sciences*, *74*, 3497–3513. https://doi.org/10.1175/jas-d-16-0376.1